Environ Monit Assess (2026) 198:86
https://doi.org/10.1007/s10661-025-14903-9

RESEARCH

Multimedia assessment of heavy metal pollution and health risks in a riverine agro-mining landscape

Charles D. Kadala · Mwemezi J. Rwiza · Grite Nelson Mwaijengo · Shovi Furaeli Sawe · Gordian Rocky Mataba

Received: 2 September 2025 / Accepted: 11 December 2025

Abstract Heavy metal pollution in agro-mining zones threatens ecosystems and human health through bioaccumulation and food-chain transfer. This study assessed heavy metal pollution and associated health risks in the Likuyu River catchment by measuring concentrations of zinc (Zn), cadmium (Cd), nickel (Ni), copper (Cu), and lead (Pb). During the rainy season, samples of water, sediment, soil, and locally cultivated vegetables were systematically collected along a 22.7 km stretch of the river. Heavy metal concentrations were analyzed by flame atomic absorption spectroscopy (FAAS), providing a multimedia view of contamination and exposure pathways. Although water showed low ionic concentrations, Cd exceeded the WHO limit (0.01 mg/L). Sediments revealed elevated Zn at Site A (108.0 mg/kg) and Ni at Site E (35.97 mg/kg), with Ni surpassing the threshold effect concentration (TEC) of 22.7 mg/kg. However, overall sediment pollution was low: Zn enrichment was slight (CF = 1.14), and a negative Igeo with PLI < 1 indicated unpolluted conditions. Soil from Site D had Ni at 107.2 mg/kg, exceeding the Tanzania Bureau of Standards (TBS) limits, with CF = 1.58 and Igeo = +0.07, indicating moderate pollution. Other sites showed CF < 1, negative Igeo, and low PLI, reflecting minimal contamination. Cowpea (*Vigna unguiculata (L.) Walp*.) and Napa cabbage (*Brassica rapa subsp. pekinensis (Lour.) Hanelt*) accumulated high levels of Ni and Pb, with Pb exceeding the Codex Alimentarius limits and Ni surpassing the European Food Safety Authority (EFSA) limits. Bioaccumulation was evident (BAF > 1), and health indices indicated noncarcinogenic (HI > 1) and carcinogenic risks (CR > 10^{-4}), especially in cowpea (CR = 0.347). Elevated Ni and Pb in soils and vegetables indicated localized exposure risks, highlighting the need for targeted monitoring, informed vegetable selection, and coordinated mitigation in agro-mining areas.

Keywords Heavy metals · Multimedia assessment · Bioaccumulation · Health risk · Agro-mining areas · Tanzania

C. D. Kadala (✉) · M. J. Rwiza · G. N. Mwaijengo · G. R. Mataba
School of Materials, Energy, Water and Environmental Sciences (MEWES), the, Nelson Mandela African Institution of Science and Technology (NM-AIST), Arusha, Tanzania
e-mail: kadalac@nm-aist.ac.tz

M. J. Rwiza
e-mail: mwemezi.rwiza@nm-aist.ac.tz

G. N. Mwaijengo
e-mail: grite.nelson@nm-aist.ac.tz

G. R. Mataba
e-mail: gordian.mataba@nm-aist.ac.tz

C. D. Kadala
Department of Natural Sciences, Mbeya University of Science and Technology (MUST), Mbeya, Tanzania

S. F. Sawe
Tanzania Atomic Energy Commission (TAEC), Arusha, Tanzania
e-mail: shovisawe@yahoo.co.uk

Published online: 05 January 2026

Introduction

Heavy metal pollution poses a significant environmental and public health threat in agro-mining landscapes. These elements are naturally occurring, characterized by relatively high density, atomic weight, or atomic number, typically with a specific gravity greater than approximately 5 g/cm^3, and include micronutrients such as zinc (Zn) and copper (Cu), alongside persistent toxic elements such as lead (Pb), cadmium (Cd), mercury (Hg), and arsenic (As), which bioaccumulate through food webs and resist degradation (Duhan et al., 2023; Kumar & Khan, 2021). Global estimates suggest that 14–17% of agricultural land exceeds safe metal thresholds, threatening food security for more than 1.4 billion people (Hou et al., 2025; Saleem et al., 2024). To understand the origins of this widespread pollution, it is essential to examine the anthropogenic drivers that increase environmental metal loads.

While naturally occurring at low concentrations, heavy metals accumulate rapidly due to anthropogenic activities. Mining operations are the dominant source in affected regions, supplemented by industrial discharge, agrochemical inputs, and vehicular emissions (Ashraf et al., 2021; Isah et al., 2024). River systems facilitate metal transport across landscapes and often serve as irrigation and domestic water sources in mining-impacted areas (Gebreyohannes et al., 2022; Mabidi et al., 2024). These pathways increase exposure risks and complicate remediation efforts.

The ecological consequences of metal pollution include water quality, soil fertility, and crop safety, especially near river corridors and mine sites (Demsie et al., 2025; Silas et al., 2024). Aquatic sediments act as both sinks and secondary sources of pollution, particularly during seasonal flooding or sediment resuspension events (Awuah et al., 2020; Njoki et al., 2024). Irrigation with polluted water introduces metals into agricultural soils and crops, reducing productivity and increasing human exposure (Lemessa et al., 2022; Sanga & Pius, 2024).

Food systems are particularly vulnerable to these impacts. Leafy vegetables, which are valued for their nutrient density, exhibit high metal uptake from polluted soils and irrigation water, posing significant exposure risks to consumers (Alegbe et al., 2025; Said et al., 2025; Telekia, 2024). Recent studies have consistently reported elevated metal concentrations in produce across diverse farming systems, with health risk assessments indicating high hazard indices and carcinogenic risks, particularly for children (Demsie et al., 2025; Hosen et al., 2024).

Comparative studies from Asia and the Pacific illustrate the variability in heavy metal pollution profiles and associated health risks across mining-impacted regions. In the Songhua River Basin, water quality remains within safety limits, but sediments and soils present moderate Cd pollution with low carcinogenic risk (Li et al., 2020). In contrast, Diarra (2022) reported elevated Pb and Cd concentrations in agricultural soils near the Vatukoula Gold Mine in Fiji, with greater ecological risks and significant health threats to children.

In East Africa, mining−agriculture interactions have raised pollution concerns (Mdachi et al., 2024; Mohammed & Nkuba, 2017). Tanzanian river systems exhibit substantial metal pollution (Mataba et al., 2016; Sawe et al., 2021). Cd levels reach 1.53 mg/kg in Mara River sediments, while in Tigithe River Pb concentrations of 17.45 mg/kg have been reported (Nkinda et al., 2021). The Ngerengere River shows elevated contamination of Cr (0.25 mg/L) and Cd (0.03 mg/L), both exceeding WHO drinking water limits (Gebreyohannes et al., 2022). Morogoro River water exhibited As concentrations of (0.47 mg/L) and Cd concentration of (0.74 mg/L). Irrigated vegetables from this area were reported to accumulate Pb and Hg (Telekia, 2024). Uranium deposits near the Mkuju River may contribute to metal contamination. Heavy metals have been detected in the surrounding soils and water (Banzi, 2016; Banzi et al., 2015, 2017). These findings highlight the need for comparative assessments across mining-impacted regions.

This study addresses one such gap by focusing on the Likuyu River catchment in northern Tanzania. Although situated 51.5 km from the Mkuju River uranium deposits, the catchment could potentially be affected by indirect pollution via atmospheric deposition, surface runoff, and groundwater flow, though direct evidence of these pathways has not been established (Dinis & Fiúza, 2021; Mitra et al., 2022; Mohammed & Mazunga, 2013; Srivastava et al., 2020). The river supports irrigation, livestock, and domestic water use, but currently lacks a comprehensive pollution assessment. Previous studies near uranium deposits have addressed broad environmental

risks, but none have conducted integrated assessments of metal pollution across the Likuyu River system (Banzi, 2016; Banzi et al., 2015, 2017; Mohammed & Mazunga, 2013), which may be affected in one way or another by ongoing mining activities that could release dust and destabilize the soil. Runoff and erosion may carry metals into rivers, threatening both ecological health and human safety (Nkinda et al., 2021). These gaps limit the understanding of pollution across environmental compartments and hinder risk evaluation.

This study hypothesizes that metal pollution in the Likuyu River catchment is increasing due to regional uranium mining activities, with significant implications for ecological integrity and human well-being. However, this study's single-season sampling design and lack of historical baseline data limit the ability to confirm temporal trends or definitively attribute sources without isotopic analysis or direct mining site characterization. Accordingly, this study was designed to (i) determine the levels of the selected metals (Ni, Cu, Zn, Cd, and Pb) in river water, sediments, agricultural soils, and leafy vegetables and evaluate risk levels via multiple indices, including the contamination factor (CF), pollution load index (PLI), and geoaccumulation index (Igeo), for soil and sediment samples. Human health risks were further assessed through the bioaccumulation factor (BAF), estimated daily intake (EDI), carcinogenic risk (CR), and hazard quotient (HQ), and (ii) the primary pollutant sources were hypothesized based on spatial and statistical evidence (multivariate statistical analysis and sediment quality guideline (SQG) thresholds). This multimedia assessment addresses existing knowledge gaps by providing detailed source apportionment analysis and risk assessment via multiple complementary methodological frameworks, providing scientific foundations for an evidence-based understanding of heavy metal pollution in mining-influenced agricultural landscapes.

Materials and methods

Study area

The study was carried out in the Likuyu River catchment, in the Ruvuma region, southern Tanzania (Fig. 1). Situated within the Namtumbo District, the river sustains diverse habitats, serves as a domestic water source for the Likuyu community, and supports irrigated agriculture and livestock keeping. The Likuyu River (about 17.642 m wide and 1.126 m deep) originates from Mchomolo Springs in Mchomolo village, flows 1.5 km south through Likuyu village, and converges with the Mwili River before draining into the Luwegu River. It lies approximately 51.5 km from the Mkuju uranium deposit (Banzi et al., 2017; Mohammed & Mazunga, 2013). The study area spans ~ 22.7 km between 10°22′51.1"S–10°14′28.9"S and 036°22′10.1"E–036°13′03.0"E. It has a rainy season (January–April, ~ 70 mm/year) and a prolonged dry season (May–December). The temperatures range from 11–29 °C during rainy months and 14–37 °C in dry months. Between December and February, prevailing winds from the uranium deposit peak at 11.6 m/s (Banzi et al., 2017; Mohammed & Mazunga, 2013). Land use includes subsistence farming (sesame, maize, Napa cabbage, cowpea, okra, pumpkin), alongside artisanal mining and wildlife conservation efforts.

Although situated near a major uranium deposit (MRP), the Likuyu River catchment remains scientifically unexamined, despite its evident susceptibility to pollution via hydrological transport, atmospheric deposition, and intensive agricultural use. Previous studies around the Mkuju uranium site have explored radioactivity and metal levels in nearby areas, but no investigation has targeted the Likuyu catchment itself, either for radiological or non-radiological pollutants across water, sediments, soils, or food crops such as leafy vegetables that are grown along the river. This study aims to fill this gap by using a multimedia approach to assess heavy metal pollution, hypothesize their sources, and assess health risks.

Sample collection

Sampling was conducted during the rainy season (April 2025) to assess spatial variations in heavy metal concentrations in the Likuyu River catchment. The literature suggests that elevated heavy metal levels in rivers, soils, and vegetables during this period are attributed to increased runoff and leaching, which poses heightened health and environmental risks. (Rahi et al., 2024).

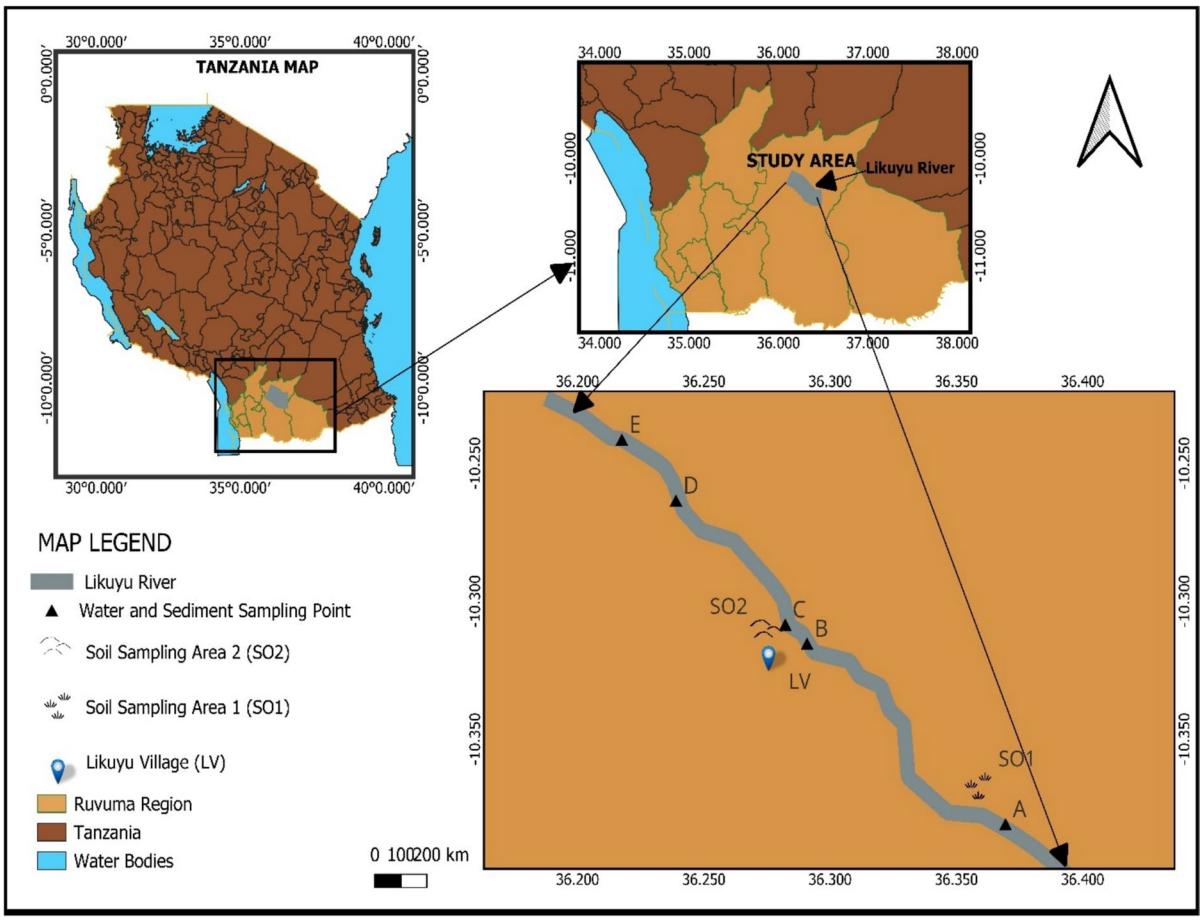

Fig. 1 Map of the study area at the national scale, with sampling points indicated, generated using QGIS version 3.44.2

Sampling of water and sediment

Surface water was collected from five designated locations (A–E) spanning about a 22.7 km segment of the river: two on the upper side, one in the middle, and two on the lower side. At each site, triplicate samples were taken from a depth of 15–20 cm using pre-cleaned, sterilized polyethylene bottles. Fifteen surface water samples were collected and preserved following an established protocol (APHA, 2022).

Similarly, triplicate sediment samples were retrieved from directly beneath the surface water sampling point at each site, at a depth of 10 cm, using a shovel while facing upstream to reduce disturbances. Fifteen samples were collected and stored in polyethylene bags. All samples were transferred to the laboratory. The shovel was cleaned before being used (APHA, 2022).

At every site, the physicochemical characteristics of the river, including electrical conductivity (EC), dissolved oxygen (DO), total dissolved solids (TDS), salinity (S), and temperature (T), were obtained using a multiparameter device (HQ 40d), while the pH level was measured with a Wagtech portable pH meter (BLE 9002). Both measurements were conducted on site. In addition, river depth was manually measured via a weighted tape marked at 10 cm intervals. At each transect point, the tape was lowered until the weight reached the riverbed, and the depth was recorded at the water surface across the river width. River width was measured by extending a tape horizontally from bank to bank, recording the distance between the water's edges on both sides. Care was taken to keep the tape taut and level to ensure accurate measurements, and the geospatial

coordinates for each sampling site were recorded via a handheld global GPS unit (Garmin Etrex 10).

Soil and vegetable sampling

Thirteen topsoil samples from the surface layer (0–20 cm) were randomly collected from agricultural fields along the river, placed in a sterilized plastic bag, and transported to laboratory for analysis in accordance to an established protocol (FAO, 2006). In addition, thirteen samples of leafy vegetables, cowpea leaves ($n=4$), pumpkin leaves ($n=3$), okra leaves ($n=3$), and Napa cabbage ($n=3$) were sampled from the fields where the soil was sampled. Non-edible parts were removed. Each sample was handled via clean gloves and sterilized tools, and placed in a labeled polyethylene bag (FAO/WHO, 2023). The scientific names of the examined leafy vegetables, provided in brackets, included: cowpea (*Vigna unguiculata (L.) Walp.*), originally described as *Dolichos unguiculatus* by Linnaeus in 1753 and later reclassified to the genus *Vigna* by Walpers in 1843; pumpkin (*Cucurbita maxima Duchesne*), validly published by Duchesne in 1786; okra (*Abelmoschus esculentus (L.) Moench*), first described as *Hibiscus esculentus* by Linnaeus in 1753 and subsequently transferred to the genus *Abelmoschus* by Moench in 1794; and Napa cabbage (*Brassica rapa subsp. pekinensis (Lour.) Hanelt*), with the species *Brassica rapa* first validly published by Linnaeus in 1753 and the subspecies originally described as *Sinapis pekinensis* by Loureiro in 1790, later reclassified as a subspecies of *B. rapa* by Hanelt in 1986 (Royal Botanic Gardens, Kew, 2025).

Heavy metal analysis

Metal concentrations (Cu, Ni, Pb, Zn, and Cd) were determined in samples of river water, sediment, soil, and leafy vegetables. Before analysis, the vegetable samples were gently washed with distilled water to remove any surface residues. All samples were subsequently air dried for 3 days to remove surface moisture and impurities manually and then in oven (60 °C–70 °C) for 48 h and homogenized using a grinder machine at the Nelson Mandela African Institution of Science and Technology (NM-AIST) laboratory, sealed in polyethylene bags, and transferred to the Geological Survey of Tanzania (GST) laboratory for heavy metal quantification.

At the GST laboratory, water samples were digested by heating with concentrated nitric acid (APHA, 2022), while powdered sediment, soil, and vegetable samples (0.50 g ± 0.02 g) were weighed and digested in aqua regia via a freshly prepared acid mixture (HNO_3: HCl, 1:3) in accordance with the established protocol for aqua regia digestion for FAAS (IOS, 1995; US EPA, 1996). Following digestion, samples were analyzed for heavy metal levels via a Varian SpectrAA-55B Atomic Absorption Spectrophotometer (Varian Inc., Australia). The levels of Cu, Ni, Pb, Zn, and Cd were quantified via calibration curves derived from reagent blanks and certified standards, with a detection limit of 0.01 ppm. The results are expressed as mg/kg for solid samples and mg/L for water samples.

Quality control

Quality control was ensured through laboratory blanks, duplicates, and matrix-specific certified reference materials (CRMs), which were analyzed alongside test samples. Analytical accuracy and precision were validated via CRMs appropriate for each matrix type.

For the geogenic matrices (soil and sediment), NCS DC 73027 (National Analysis Center for Iron & Steel [NACIS], Beijing, China) was employed. The recovery rates ranged from 95 to 99%, with relative standard deviations (RSDs) between 1 and 6%, meeting the accepted analytical performance criteria (recoveries: 80–120%; RSD: < 5%) and confirming the reliability of the method for heavy metal quantification. For the biological matrices (leafy vegetables), NCS ZC73018/NIM-GBW 100220 (NACIS, Beijing, China), derived from citrus leaves, was used. Its certified analyte profile aligns with plant tissue composition, supporting its application in dietary exposure assessments. The measured concentrations of Zn, Cd, Ni, Cu, and Pb yielded recoveries between 81.8% and 116.1%, with RSDs ranging from 7.6% to 11.8%, which is consistent with the expected variability in biological matrices.

Only high-purity reagents were employed, and all instruments were calibrated using certified reference standards for metal analysis. Calibration blanks and independent verification standards were

analyzed after every five samples to confirm instrument stability. Procedural and field blanks showed no detectable contamination (< 0.01 ppm), and matrix interference remained below 1% for all the elements. These results affirm the precision and accuracy of the method for heavy metal determination in both geogenic and biological matrices.

Statistical analysis

Spatial variation in heavy metal concentrations across sampling sites was evaluated via analysis of variance (ANOVA), with Tukey's HSD and Kruskal–Wallis tests applied as appropriate for post hoc and nonparametric comparisons. Relationships among metals were explored via both Pearson and Spearman correlation coefficients. To uncover the underlying pollution structures, principal component analysis (PCA) and hierarchical clustering were employed. All the statistical procedures were conducted in R (v4.5.0; R Core Team, 2025).

Ecological risk interpretation was guided by sediment quality guidelines (SQGs), which incorporate crustal background concentrations (CBCs), threshold effect concentrations (TECs), probable effect concentrations (PECs), and national benchmarks from the Tanzania Bureau of Standards (TBSs). For consistency in the statistical treatment, values below the detection limits (BDLs) were conservatively assigned as half the detection threshold.

Assessment of metal concentration in soil and sediment

To examine the extent of metal pollution in the soil and river sediment, three indices were applied: the geoaccumulation index (Igeo), contamination factor (CF), and pollution load index (PLI). Reference concentrations for the metals analysed in this study were based on average shale values representing crustal material in mg/kg: Cd (0.3), Ni (68), Pb (20), Zn (95), and Cu (45) (Turekian & Wedepohl, 1961).

Geoaccumulation index

The geoaccumulation index (Igeo) was applied to quantify metal pollution levels in soil and sediment samples. It was computed using Eq. 1, established by Müller, (1979):

$$I_{geo} = log_2\left(\frac{c}{1.5 \times B}\right) \quad (1)$$

where C represents the measured concentration of the metal and B denotes its geochemical background concentrations (mg/kg), for this study, the values used were Cd (0.3), Ni (68), Pb (20), Zn (95), and Cu (45) adopted from Turekian and Wedepohl (1961). The constant 1.5 accounts for natural lithogenic variability.

Igeo values are categorized into seven distinct classes: Class 0 (≤0): indicates no pollution; Class 1 (0–1): ranges from clean to slightly polluted; Class 2 (1–2): reflects moderate contamination; Class 3 (2–3): suggests moderate to strong pollution; Class 4 (3–4): denotes strong pollution; Class 5 (4–5): represents strong to extreme pollution; and Class 6 (≥5): signifies extremely high pollution level (Nur-E-Alam et al., 2022).

Contamination factor

To evaluate the degree of pollution linked to individual heavy metals, the contamination factor (CF) was calculated using Eq. 2.

$$CF = \frac{C}{B} \quad (2)$$

where C and B represents the measured concentration of the metal and its geochemical background concentrations, respectively. According to Hakanson (1980), CF values were interpreted as follows: less than 1 indicates minimal pollution; values between 1 and 3 reflect moderate levels; those ranging from 3 to 6 suggest substantial contamination; and values equal to or exceeding 6 denote severe pollution (Isah et al., 2024; Nur-E-Alam et al., 2022).

Pollution load index

The pollution load index (PLI) provides an overall measure of pollution and was calculated using Eq. 3 as follows:

$$PLI = \left(CF_1 \times CF_2 \times CF_3 \times \ldots CF_n\right)^{1/n} \quad ((3))$$

where CF_1 to CF_n are the pollution factors for each metal, and n is the number of metals analyzed. The PLI offers a simple metric to compare metal pollution levels and are categorized as follows: values below 1 indicate an unpolluted state; values between 1 and 2 reflect moderate contamination; those ranging from 2 to 3 signify heavy pollution; and values exceeding 3 denote extremely high pollution levels (Pal & Maiti, 2018; Rahi et al., 2024).

Bioaccumulation factor

The bioaccumulation factor (BAF) was used to quantify metal transfer from the soil to the vegetables. BAF was computed using Eq. 4.

$$BAF = \frac{C_{veg}}{C_{soil}} \quad (4)$$

Where C_{veg} is the metal concentration in the vegetable tissue and C_{soil} in the corresponding soil (Kazemi et al., 2022; Osae et al., 2023).

Human health risk assessment

Potential health risks associated with polluted vegetables were assessed via the model developed by Romero-Estévez et al. (2019). Indicators such as estimated daily intake (EDI), hazard quotient (HQ), hazard index (HI), and carcinogenic risk (CR) were applied for adult exposure (Galarza et al., 2023; Kazemi et al., 2022).

Estimated daily intake

The estimated daily intake (EDI) (mg/kg/day) of heavy metals was calculated basing on metal concentrations in vegetables (mg/kg) and average daily consumption rates (kg/day) using Eq. 5 as follows:

$$EDI = \frac{C \times IR}{BW} \quad (5)$$

where C is the metal concentration in vegetables (mg/kg), IR is the ingestion rate (0.2 kg/day), and BW is the average adult body weight (70 kg) (Mustatea et al., 2021; USEPA, 2011).

Hazard quotient

The hazard quotient (HQ) was used to evaluate noncarcinogenic risk, calculated using Eq. 6.

$$HQ = \frac{EDI}{RD} \quad (6)$$

where the EDI is the estimated daily intake and RD is the reference dose (mg/kg/day). The RD values used were 0.001 for Cd, 0.0035 for Pb, 0.3 for Zn, 0.04 for Cu, and 0.02 for Ni (Osae et al., 2023; USEPA, 2011).

Hazard index

The aggregate noncarcinogenic risk posed by multiple metals was quantified as the sum of all individual hazard quotients (HQs). An HI value less than 1 reflects minimal noncarcinogenic risk, while values greater than 1 indicate a potential for health-related effects (Galarza et al., 2023; Osae et al., 2023).

Carcinogenic risk

Carcinogenic risk (CR) estimates lifetime cancer risk and was calculated using Eq. 7 as follows:

$$CR = EDI \times CSF \quad (7)$$

where CSF is the cancer slope factor (mg/kg/day)$^{-1}$. The CSF values used were from USEPA (2011): 0.38 for Cd, 1.7 for Ni, and 0.0085 for Pb. The risk thresholds for carcinogenic exposure were interpreted as follows: $CR > 1 \times 10^{-4}$ indicates unacceptable risk; $CR < 1 \times 10^{-6}$ is considered negligible; and values between 1×10^{-6} and 1×10^{-4} fall within the acceptable range (Osae et al., 2023; USEPA, 2011).

Results and discussion

Hydro chemical characteristics of the Likuyu River

Analysis of physicochemical parameters in the Likuyu River revealed marked spatial variability across the five sampling locations (Table 1). Generally, the river exhibited slightly alkaline conditions (pH 7.03–7.42) and low salinity (0.07–0.08 ‰), characteristics typical of tropical freshwater systems. Statistical tests; ANOVA (F) and Kruskal–Wallis (χ^2) indicate spatial variation across sites (Table 1). Electrical conductivity (EC), total dissolved solids (TDS), and temperature

Table 1 Summary of descriptive statistics for physicochemical parameters of water in the Likuyu River across sampling sites (A–E) expressed as the means ± SDs with ranges in parentheses

Site	pH[b]	EC (µs/cm)[a]	DO (mg/L)[b]	TDS (mg/L)[a]	S (‰)	T (°C)[a]
A	7.03 ± 0.41 (6.56–7.30)	160.43 ± 2.16 (158.4–162.7)	6.13 ± 0.2 (5.96–6.35)	76.67 ± 0.31 (76.4–77.0)	0.08 ± 0 (0.08–0.08)	23.8 ± 0.17 (0.08–0.08)
B	7.34 ± 0.23 (7.20–7.60)	153.13 ± 0.06 (153.1–153.2)	6.72 ± 0.02 (6.71–6.74)	72.67 ± 0.29 (72.5–73.0)	0.07 ± 0 (0.07–0.07)	23.43 ± 0.35 (23.1–23.8)
C	7.25 ± 0.1 (7.13–7.31)	150.53 ± 0.64 (149.8–150.9)	6.62 ± 0.01 (6.61–6.63)	71.3 ± 0.17 (71.1–71.4)	0.07 ± 0 (0.07–0.07)	24.3 ± 0.17 (24.2–24.5)
D	7.23 ± 0 (7.23–7.23)	149.6 ± 0 (149.6–149.6)	6.5 ± 0 (6.50–6.50)	70.8 ± 0 (70.8–70.8)	0.07 ± 0 (0.07–0.07)	25 ± 0 (25.0–25.0)
E	7.42 ± 0.1 (7.31–7.48)	150.67 ± 0.29 (150.5–151.0)	6.66 ± 0 (6.66–6.66)	71.1 ± 0 (71.1–71.1)	0.07 ± 0 (0.07–0.07)	26.83 ± 0.4 (26.6–27.3)
F, p	6.92, 0.006	34.18, < 0.001	15.74, < 0.001	35.46, < 0.001	91.89, < 0.001	128.35, < 0.001
X^2, *p*	11.06, 0.026	13.71, 0.008	13.24, 0.010	13.71, 0.008	13.71, 0.008	13.71, 0.008
WHO*	6.5–8.5	1400	5	1000	NA**	25

*WHO Guidelines for Drinking-Water Quality (Wang et al., 2022; WHO, 2022); **NA = Not available

[a]Means highly significant difference ($p < 0.001$); [b]Means moderate significant difference ($p < 0.05$)

showing highly significant differences among sites ($p < 0.001$), whereas pH and dissolved oxygen (DO) exhibited moderate variation ($p < 0.05$). Salinity showed minimal variation, with Location A having slightly higher salinity levels.

Site A presented distinct physicochemical attributes of water, with significantly greater EC (160.43 ± 2.16 µS/cm), TDS (76.67 ± 0.31 mg/L), and salinity (0.08 ‰) values than the other sites did ($p < 0.001$). Concurrently, this site presented reduced DO levels (6.13 ± 0.2 mg/L, $p < 0.01$), suggesting ionic enrichment coupled with oxygen depletion. These conditions likely result from anthropogenic influences, particularly agricultural runoff and domestic discharge, as evidenced by the site's proximity to human settlements, irrigated croplands, and areas with intensive livestock activity observed during fieldwork. Similar patterns of ionic enrichment and oxygen depletion have been documented in the Tajan River, where agricultural activities significantly altered water chemistry (Farjoudi & Alizadeh, 2021). In contrast, Site E presented the highest temperature (27.3 °C, $p < 0.001$) and elevated pH relative to those of Site A ($p = 0.041$) while maintaining moderate ionic concentrations, as this point is where the Likuyu River converges with the Mwili River. The elevated temperature at this site likely contributes to reduced oxygen solubility, creating the thermal stress conditions common in tropical river systems (Rajesh & Rehana, 2022; Zhang et al., 2024). Sites B–D formed an intermediate cluster with moderate values across all parameters, suggesting relatively stable conditions.

Correlation analysis revealed strong positive associations among EC, TDS, and salinity ($r \geq 0.93$), indicating a common source of dissolved substances (Fig. 2). This relationship suggests that ionic enrichment across the river system originates from similar anthropogenic sources, which is consistent with findings from the Mara River Basin, where agricultural and domestic activities created comparable water quality indicators (Kimario et al., 2025). The weak correlation between pH and DO ($r = 0.30$) and the limited association between temperature and DO ($r = 0.27$) indicate that the thermal influences on oxygen dynamics are moderate in this system.

Principal component analysis (PCA) revealed two dominant environmental gradients, ionic load and thermal stress, explaining 82.9% of the overall variance in water quality parameters (Fig. 3). Dim1 explains 69% of the overall variance and is influenced by EC, TDS, and salinity, whereas Dim2 accounts for 13.9% and is shaped by temperature and pH. This analysis clearly separated Site A as a high-ionic/low-DO environment, Site E as thermally distinct, and Sites B–D as representing moderate conditions. Regression modeling further supported these relationships, with temperature and pH serving as significant predictors of DO ($R^2 = 0.71$) and EC serving as

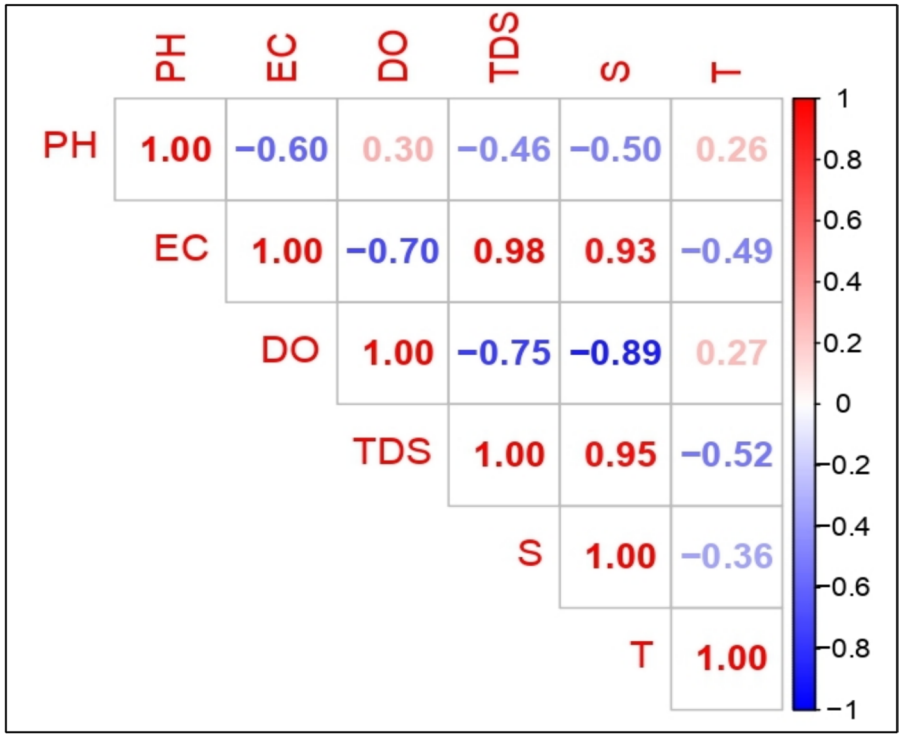

Fig. 2 Pearson correlation heatmap of physicochemical parameters of water samples from the Likuyu River

strong predictors of TDS ($R^2 = 0.90$). These models reinforce the importance of ionic and thermal factors in controlling water chemistry dynamics in the Likuyu River system.

All analyzed heavy metals were below detection limits (BDLs) and complied with WHO standards (Table 2). This pattern suggests effective sediment binding of metals and limited anthropogenic metal inputs to the water column, which is consistent with observations in other East African river systems (Gebreyohannes et al., 2022; Mataba et al., 2016). However, the detection limit for cadmium (0.01 mg/L) exceeds the WHO guideline (0.003 mg/L). Continuous monitoring is recommended, given Cd's persistence and potential bioaccumulation (Kubier et al., 2019; Mdachi et al., 2024).

The water quality parameters exhibited clear spatial heterogeneity across the sites. Elevated agricultural runoff and domestic discharge were observed near Site A, whereas Site E presented distinct thermal anomalies associated with convergence with the Mwili River. Cd concentrations require continued monitoring due to potential contamination risks. Strong correlations among ionic parameters and pollution source patterns were effectively identified through multivariate analysis. Seasonal variation and environmental shifts remain key areas for future investigations.

Although the physicochemical profile of the Likuyu River generally complies with WHO guidelines, localized stress at Sites A and E raises concerns about long-term water security and ecosystem health. Ionic enrichment and oxygen depletion at Site A, coupled with thermal stress at Site E, may compromise aquatic biodiversity and alter ecosystem functioning. Variations in pH, temperature, and ionic strength can influence metal speciation and mobility, potentially increasing heavy metal bioavailability under future anthropogenic or climate-driven scenarios. The presence of a uranium mining site approximately 52 km from the study area further underscores the need to consider broader environmental influences on heavy metal dynamics.

Heavy metal distribution in river sediments

Statistical test results (ANOVA F, p and Kruskal–Wallis χ^2, p) for heavy metal analysis of sediment samples from the Likuyu River revealed significant spatial heterogeneity, with Zn, Ni, and Pb showing statistically significant variation across sampling sites

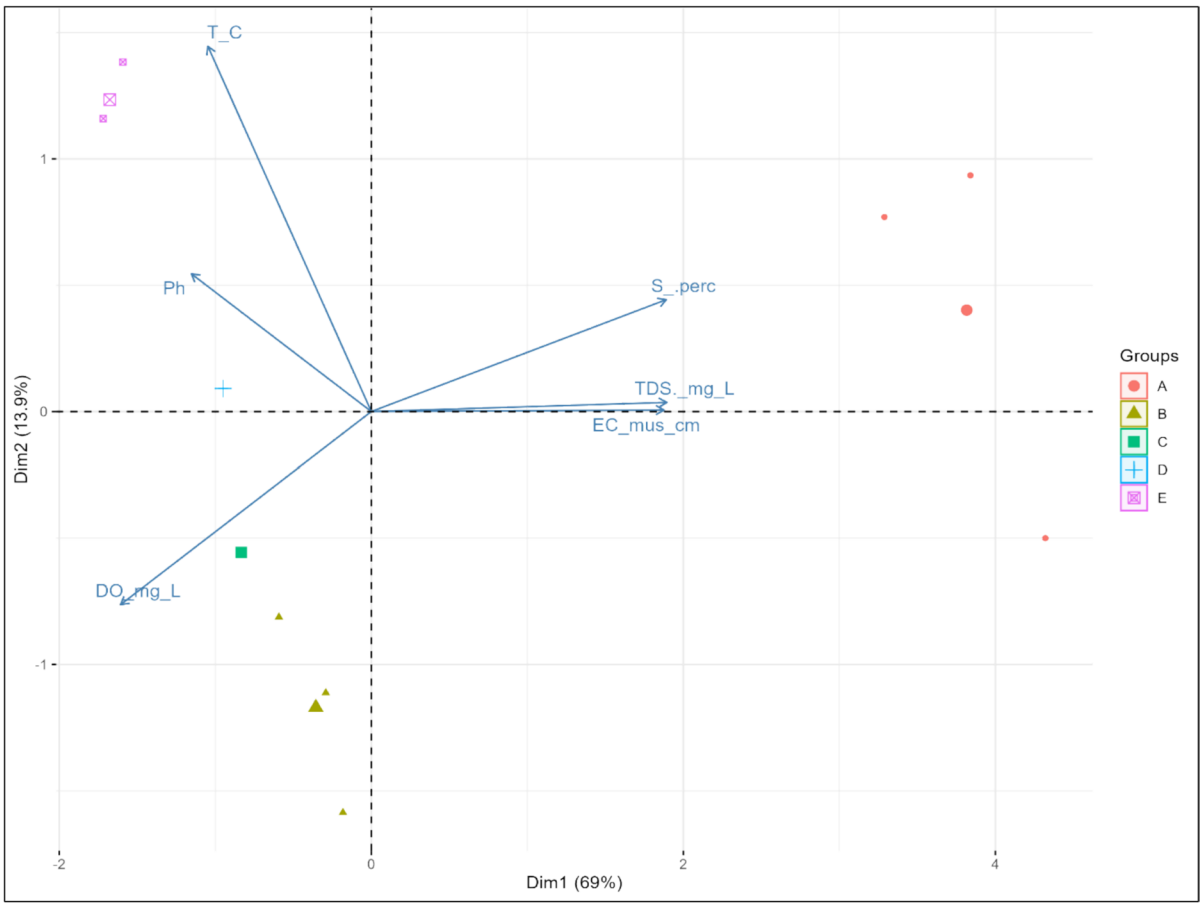

Fig. 3 PCA plot showing the distribution of sampling zones (A–E) and the contributions of physicochemical parameters to the first two principal components. The arrows represent variable loadings, indicating the direction and magnitude of influence

Table 2 Measured levels of heavy metals (mg/L) in Likuyu River water samples and corresponding WHO guideline values (2022)

Parameter	Statistic			*WHO standards
	Min	Max	Mean	
Zn (mg/L)	BDL	BDL	BDL	3–5
Cd (mg/L)	BDL	BDL	BDL	0.003
Ni (mg/L)	BDL	BDL	BDL	0.07
Cu (mg/L)	BDL	BDL	BDL	2.0
Pb (mg/L)	BDL	BDL	BDL	0.01

*WHO Guidelines for Drinking-Water Quality (WHO, 2022)

A–E ($p=0.0087$, $p=0.0319$, and $p=0.0394$, respectively; Table 3). This spatial distribution pattern suggests localized pollution sources rather than uniform background enrichment throughout the river system.

Site A had the highest Zn concentration (108.0 ± 65.9 mg/kg), which was above the crustal background (71 mg/kg) and approached the threshold effect concentration (TEC) of 121 mg/kg. This elevation indicates moderate localized enrichment, potentially attributed to surface runoff and domestic activities based on field observations and spatial patterns, though direct source confirmation was not conducted. This is consistent with anthropogenic influences observed in other Tanzanian river

Table 3 Concentrations of heavy metals (Zn, Ni, Cu, Pb, and Cd) (mg/kg) in the Likuyu River sediment across the sampling sites (A–E), expressed as the means ± SDs with ranges in parentheses, and the pollution load index (PLI) values

Site	Zn	Ni	Cu	Pb	Cd	PLI
A	108.0 ± 65.9 (53–181)	32.1 ± 26.9 (1.1–49.7)	2.23 ± 0.38 (1.8–2.5)	12.87 ± 7.36 (4.9–19.4)	BDL	0.251
B	8.5 ± 1.25 (7.1–9.5)	3.9 ± 1.93 (2.2–6.0)	2.73 ± 0.71 (2.1–3.5)	4.30 ± 0.70 (3.6–5.0)	BDL	0.077
C	9.5 ± 2.50 (7.5–12.3)	7.5 ± 2.33 (5.6–10.1)	5.17 ± 3.65 (1.6–8.9)	3.00 ± 1.40 (1.6–4.4)	BDL	0.097
D	17.73 ± 4.40 (12.9–21.5)	12.03 ± 3.72 (7.8–14.8)	6.60 ± 5.28 (3.5–12.7)	5.07 ± 2.19 (2.6–6.8)	BDL	0.143
E	16.17 ± 1.59 (15.2–18.0)	35.97 ± 6.51 (29.0–41.9)	4.13 ± 1.55 (3.0–5.9)	4.27 ± 0.78 (3.4–4.9)	BDL	0.148
(*F, p*)	6.26,**0.0087**[a]	4.11, **0.0319**[a]	1.08, 0.418	3.80, **0.0394**[a]	NA	
(X^2, *p*)	12.23,**0.0157**	6.93, 0.1395	6.04, 0.1959	6.65, 0.1554	NA	
CBC*	71	47	25	20	0.1	
TEC**	121	22.7	31.6	35.8	0.99	
PEC**	459	48.6	149	128	4.98	

*Crustal background concentrations (CBCs) in the continental crust (Mataba et al., 2016; Wedepohl, 1995)

** Consensus-based sediment quality guidelines (SQGs) (MacDonald et al., 2000; Mataba et al., 2016)

[a]Indicate highly significant differences ($p < 0.01$) according to ANOVA

[b]Statistically significant differences ($p < 0.05$) according to the Kruskal−Wallis test

BDL below detection limits and *NA* not applicable

systems (Gebreyohannes et al., 2022; Mataba et al., 2016). While these concentrations remain lower than those reported in heavily impacted systems in Kenya, Nigeria, and Pakistan (Ashraf et al., 2021; Edogbo et al., 2020; Njoki et al., 2024). They nevertheless represent a potential ecological concern that warrants monitoring.

Ni concentrations presented the most significant ecological concern, with Sites A (32.1 ± 26.9 mg/kg) and E (35.97 ± 6.51 mg/kg) exceeding the TEC threshold of 22.7 mg/kg but remaining below the probable effect concentration (PEC) of 48.6 mg/kg (MacDonald et al., 2000; Mataba et al., 2016). These elevated levels suggest potential adverse effects on benthic organisms and may result from natural mineral weathering, agricultural inputs, or localized anthropogenic activities. Similar Ni enrichment patterns have been documented in comparable East African river systems, often attributed to the weathering of ultramafic rocks and agricultural intensification (Nkinda et al., 2021).

The Pb concentrations were highest at Site A (12.87 ± 7.36 mg/kg), remaining below the established regional benchmarks but indicating localized anthropogenic influence. Despite these moderate levels, the well-documented toxicity and potential for bioaccumulation of Pb in aquatic food webs make it a priority pollutant for continued monitoring (Mabidi et al., 2024; Silas et al., 2024). In contrast, Cu levels remained consistently low across all sites (mean = 4.17 mg/kg), well below the TEC of 31.6 mg/kg and consistent with regional baseline concentrations, suggesting minimal ecological risk (Gebreyohannes et al., 2022). Cd was below the detection limits (< 0.01 mg/kg) at all the sites, reflecting the natural background conditions typical of similar river systems (Edogbo et al., 2020; Mataba et al., 2016).

Correlation analysis revealed distinct clustering patterns among heavy metals, providing insights into pollution sources and geochemical behavior (Fig. 4). The strong positive associations of Zn–Pb ($r = 0.622$, $p = 0.0132$) and Ni–Pb ($r = 0.673$, $p = 0.006$) suggest comobilization through shared pollution from human activities, notably domestic effluent, agricultural runoff, and atmospheric deposition. This association pattern is characteristic of mixed pollution sources common in river systems subjected to anthropogenic pressures (El Mrissani et al., 2021). Cu exhibited weak and negative correlations with other metals (Cu–Zn: $r = -0.231$), indicating that a

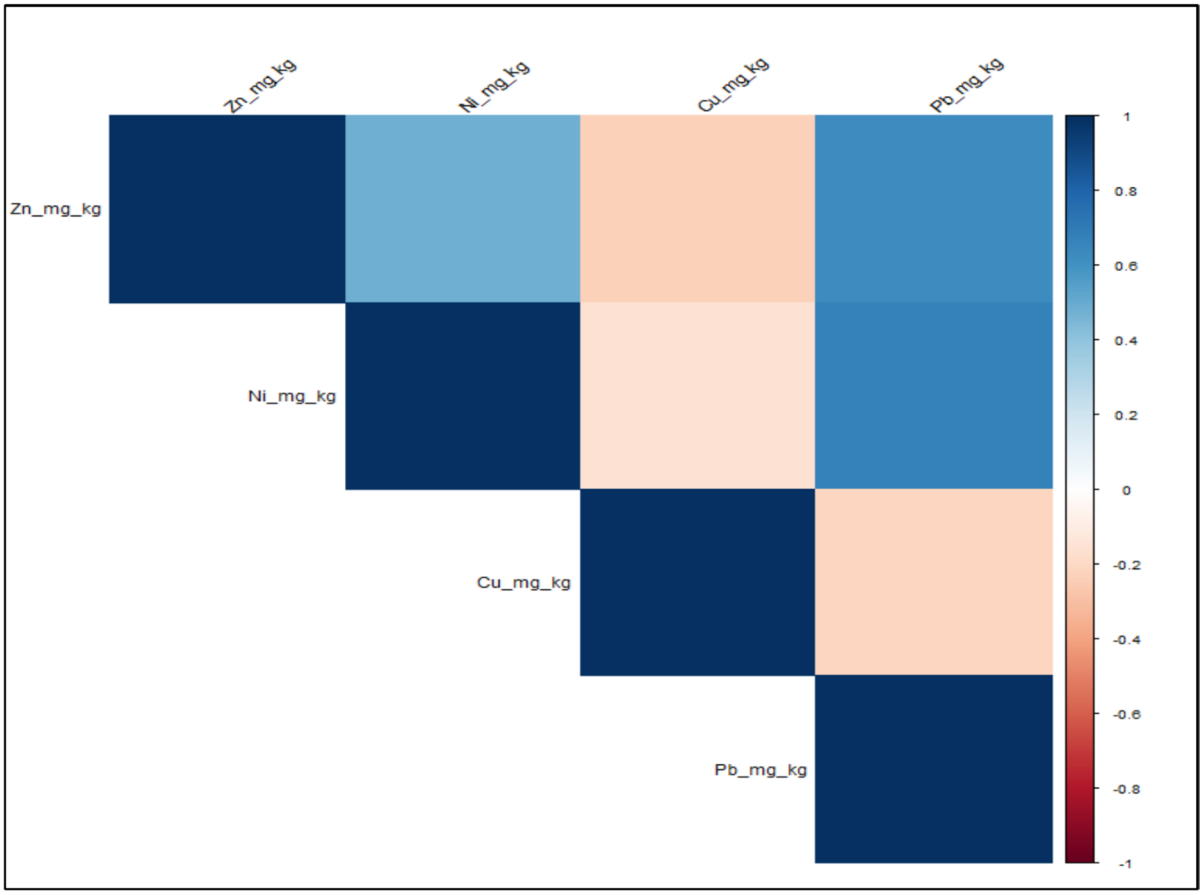

Fig. 4 Pearson correlation heatmap of heavy metals in river sediment samples

distinct geochemical origin was likely tied to natural background levels or isolated agricultural inputs. This contrasting behavior reinforces the spatial heterogeneity of the metal distribution and suggests different transport and deposition mechanisms for Cu than for the Zn-Ni-Pb cluster.

Principal component analysis further supported these relationships, with Dim1 (explaining 57.1% of the variance) loading strongly on Zn, Ni, and Pb (−0.538, −0.543, and −0.589, respectively), whereas Dim2 (22.8% of the variance) was dominated by Cu (−0.955; Fig. 5). This multivariate structure clearly distinguishes between the main contamination axis (PC1) and the distinct Cu signature (PC2), providing statistical support for the identified source differentiation.

The pollution indices generally revealed low pollution levels across the Likuyu River system, with localized enrichment at specific sites. The contamination factor (CF) for Zn at Site A reached 1.14, indicating moderate pollution, whereas the other metals remained below the pollution thresholds (CF < 1) (Fig. 6a). The geoaccumulation index (Igeo) values were negative across all the metals (−5.49 for Cd to −0.40 for Zn), indicating that the sediments were unpolluted according to established criteria (Fig. 7b). These results align with pollution assessments from the Mara and Thiba Rivers, which similarly exhibit minimal overall enrichment despite localized hotspots (Nkinda et al., 2021; Silas et al., 2024). The PLI ranged from 0.077 at Site B to 0.251 at Site A, with all sites falling below the threshold of 1.0 (Table 3), which would indicate progressive deterioration. However, the threefold difference between the minimum and maximum PLI values underscores the spatial variability in

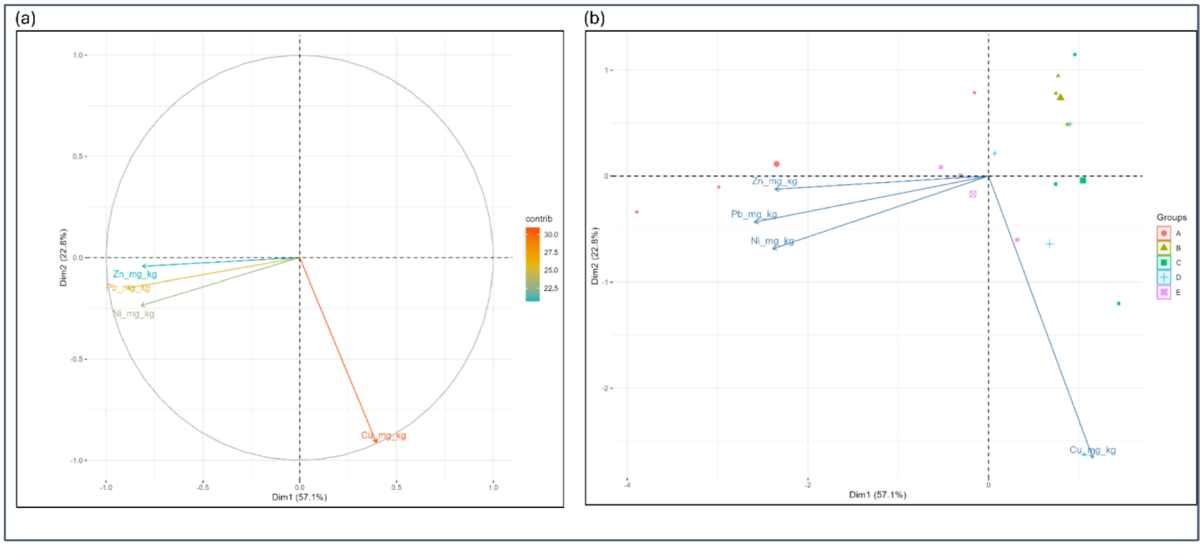

Fig. 5 PCA biplots showing the contributions of metal variables to the first two components and the clustering of sediment samples. The first two components account for 79.9% of the total variance (Dim1: 57.1%, Dim2: 22.8%). (**a**) shows the correlation circle, where the vector length and direction indicate the strength and orientation of each variable's contribution to the principal components, and (**b**) displays sample groupings on the basis of PCA scores, with distinct clusters corresponding to different sampling categories

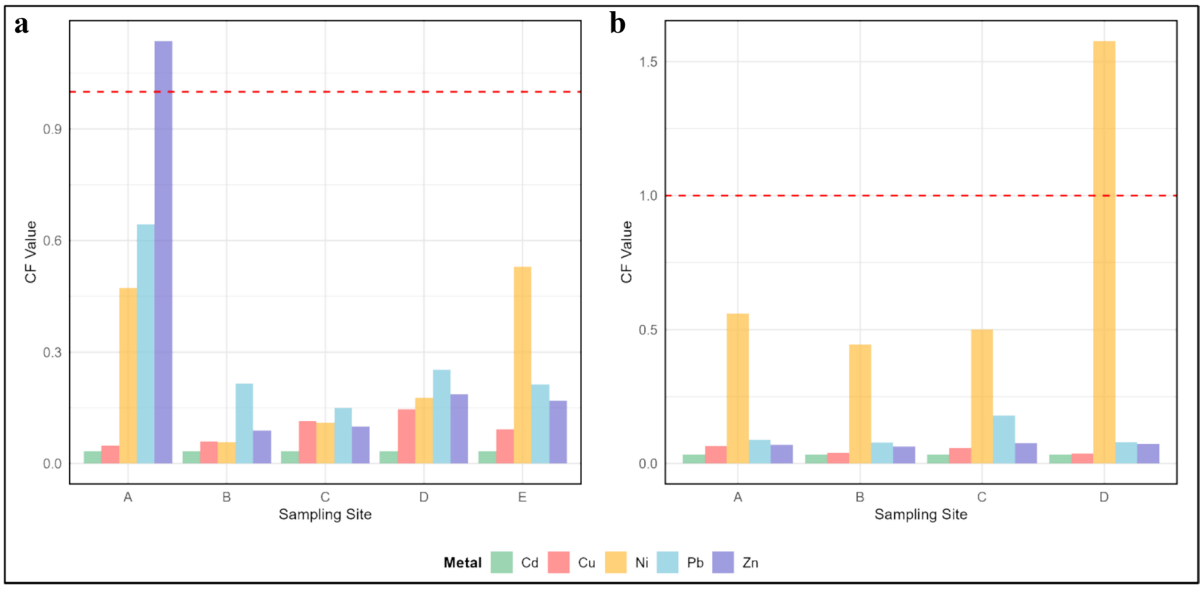

Fig. 6 CF values of Zn, Cd, Ni, Cu, and Pb in (a) river sediment (left) and (b) agricultural soil samples(right)

contamination patterns and the need for site-specific management approaches.

Despite generally acceptable pollution levels, the ecological implications of elevated Zn, Ni, and Pb concentrations at Sites A and E require careful consideration. Ni concentrations above TEC thresholds may cause sublethal effects in benthic communities, including reduced species diversity and altered community structure, as observed in similar systems in Bangladesh, where comparable metal levels disrupt

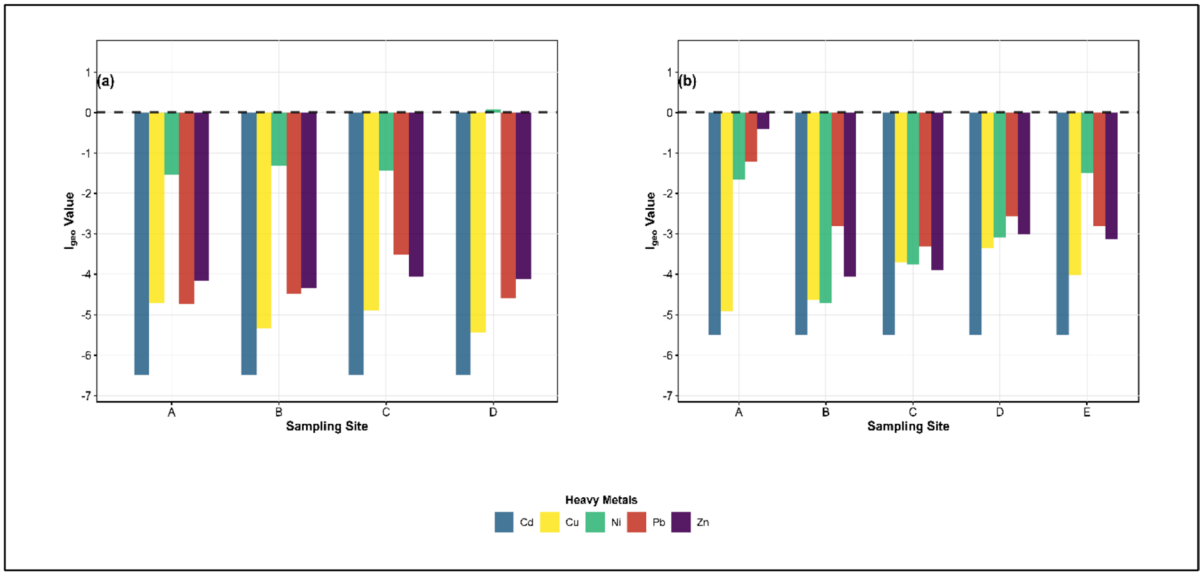

Fig. 7 Igeo values of heavy metals in (a) agricultural soil and (b) river sediment

sediment-dwelling fauna (Hosen et al., 2024). The long-term retention of these metals in sediment acts as a persistent pollution source, driven by their strong binding to clay particles and organic matter under the neutral and oxygen-rich conditions typical of the Likuyu River (Wang et al., 2022).

The sediment-bound nature presents both current and future environmental concerns. Under dynamic environmental conditions, such as flooding, sediment disruption, or chemical shifts, metals previously sequestered in sediments may re-enter the water column, increasing their accessibility to biota and increasing potential exposure across affected ecosystems (Silas et al., 2024; Wang et al., 2022).

The clustering of Zn, Ni, and Pb at Sites A and E creates ecological hotspots where metal bioaccumulation in benthic organisms may disrupt aquatic food webs. In particular, Pb poses significant risks owing to its neurological and reproductive toxicity even at sublethal concentrations. Localized enrichment of Zn, Ni, and Pb at Sites A and E indicates areas for continued observation and possible management intervention if trends persist.

Heavy metal levels in agricultural soils

The agricultural soils along the Likuyu River presented distinct spatial heterogeneity in terms of heavy metal concentrations (Table 4). Ni concentrations ranged from 30.3 mg/kg at Site B to 107.20 mg/kg at Site D, with the latter exceeding the Tanzania Bureau of Standards limit of 50 mg/kg. Statistical test results (ANOVA F, p and Kruskal−Wallis χ^2, p) confirmed significant intersite differences for Ni ($F = 108.8$, $p < 0.001$) and Cu ($F = 7.652$, $p = 0.0076$), whereas Zn, Pb, and Cd showed no significant spatial variation.

The Cu concentration varied from 1.70 mg/kg at Site D to 2.97 mg/kg at Site A, reflecting localized enrichment processes. This spatial variability aligns with findings of Telekia (2024) in agricultural areas of the Morogoro River, where Cu concentrations (1.2–4.8 mg/kg) were correlated with fertilizer application patterns. The irregular Cu distribution suggests that site-specific agronomic practices, such as micronutrient applications or copper-based fungicides, influence local concentrations. Zn (5.98–7.27 mg/kg), Pb (1.60–3.57 mg/kg), and Cd (<0.01 mg/kg) showed uniform distributions across sites, with all values well below regulatory limits. These patterns indicate limited anthropogenic input and predominant natural background levels. The consistently low Cd concentrations confirmed that minimal Cd was present in the agricultural soils of the region.

Correlation analysis (Fig. 8) revealed one significant relationship: Zn and Pb were positively

Table 4 Concentrations of Zn, Ni, Cu, Pb, and Cd (mg/kg) in agricultural soil across sampling sites (A–D), expressed as the means ± SDs with ranges in parentheses, and the PLI values are included for each site

Site	Zn	Ni	Cu	Pb	Cd	PLI
A	6.63 ± 1.43 (5.4–8.2)	38.1 ± 10.1 (29.8–49.4)	2.97 ± 0.23 (2.7–3.1)	1.83 ± 1.45 (0.4–3.3)	BDL	0.096
B	5.98 ± 1.07 (4.7–7.3)	30.3 ± 6.44 (25.5–39.8)	1.78 ± 0.13 (1.6–1.9)	1.80 ± 0.55 (1.4–2.6)	BDL	0.078
C	7.27 ± 1.15 (6.1–8.4)	34.1 ± 2.45 (31.6–36.5)	2.60 ± 0.70 (1.9–3.3)	3.57 ± 1.15 (2.4–4.7)	BDL	0.105
D	6.90 ± 0.20 (6.7–7.1)	107.2 ± 1.40 (106–109)	1.70 ± 0.40 (1.3–2.1)	1.60 ± 0.50 (1.1–2.1)	BDL	0.103
(*F*, *p*)	0.923, 0.468	108.8, < **0.001**[a]	7.652, **0.0076**[a]	2.804, 0.101	NA	
(X^2, *p*)	2.65, 0.449	7.82, **0.0499**[b]	8.07, **0.0447**[b]	5.01, 0.171	NA	
TBS*	150.0	50.0	200.0	200.0	1.000	

*TBS maximum allowable limit for heavy metals in soil (Tanzania Bureau of Standards, 2007)

[a]Indicate highly significant differences ($p < 0.01$) according to ANOVA

[b]Means statistically significant differences ($p < 0.05$) according to the Kruskal−Wallis test

correlated ($r = 0.618$, $p = 0.0244$), suggesting shared contamination sources or geochemical behavior. This pattern mirrors results in Ethiopian agricultural soils, where the Zn−Pb correlation (r = 0.72, $p < 0.01$) was attributed to phosphate fertilizer impurities and atmospheric deposition (Demsie et al., 2025). Other metal pairs showed weak to moderate associations without statistical significance, indicating independent input pathways.

The first two principal components (Fig. 9) accounted for 79.6% of the overall variance in the dataset. Dim1 (49.9% variance) was dominated by Pb (–0.622), Cu (–0.522), and Zn (–0.497), reflecting agricultural inputs such as fertilizers and soil amendments. Dim2 (29.7% variance) was driven by Ni (–0.758) and Zn (–0.585), suggesting shared pollution sources likely geological or mining-related sources. The distinct geochemical behavior of Ni in Dim2, combined with its spatial confinement to Site D, indicates geological or extractive influences rather than agricultural sources. Banzi et al. (2017) documented similar patterns around the Mkuju River uranium project, where Ni concentrations (15–89 mg/kg) correlated with uranium-bearing geological formations. Field observations at Site D suggest that phosphate fertilizer inputs and weathering of mineral-rich parent material may have contributed to the elevated Ni concentrations (45.2 mg/kg) in phosphate tailings from the Minjingu Mines, as supported by Mdachi et al. (2024). However, without fertilizer application records, parent material geochemical analysis, or comparison with unfertilized control sites, these remain plausible hypotheses rather than confirmed sources.

Site D presented an elevated CF (1.577) (Fig. 6b) and positive Igeo (+0.07) for Ni, indicating moderate pollution (Fig. 7a). The other sites maintain CF < 1 and negative Igeo values, which are consistent with background conditions. These values align with those reported by Sanga and Pius (2024) for contaminated Tanzanian soils (CF = 1.2 to 2.1, Igeo = 0.1 to 0.9). The PLI values ranged from 0.078 to 0.105 across all the sites (Table 4), indicating minimal cumulative pollution despite the localized Ni anomaly. These PLI values are less than the values observed by Sabijon et al. (2024) for agricultural soils in the floodplains of the Taft River Basin, Philippines, where mining-impacted sites exhibited moderate to high contamination (PLI > 1.0), confirming relatively low overall contamination in the Likuyu system.

It is important to note that elevated Ni levels were confined to Site D and do not represent generalized contamination across the study area. These results demonstrate that agricultural soils along the Likuyu River generally maintained acceptable metal concentrations during the rainy season sampling period, with Site D representing an isolated pollution hotspot that warrants specific attention to assess temporal stability and potential expansion via surface runoff or groundwater transport. The contrast between Site D and the other sites (B and C) provides a framework for distinguishing anthropogenic impacts from natural variations in future monitoring programs.

Heavy metal levels in edible leafy vegetables

Measured levels of heavy metals varied significantly across the sampling sites and vegetable types,

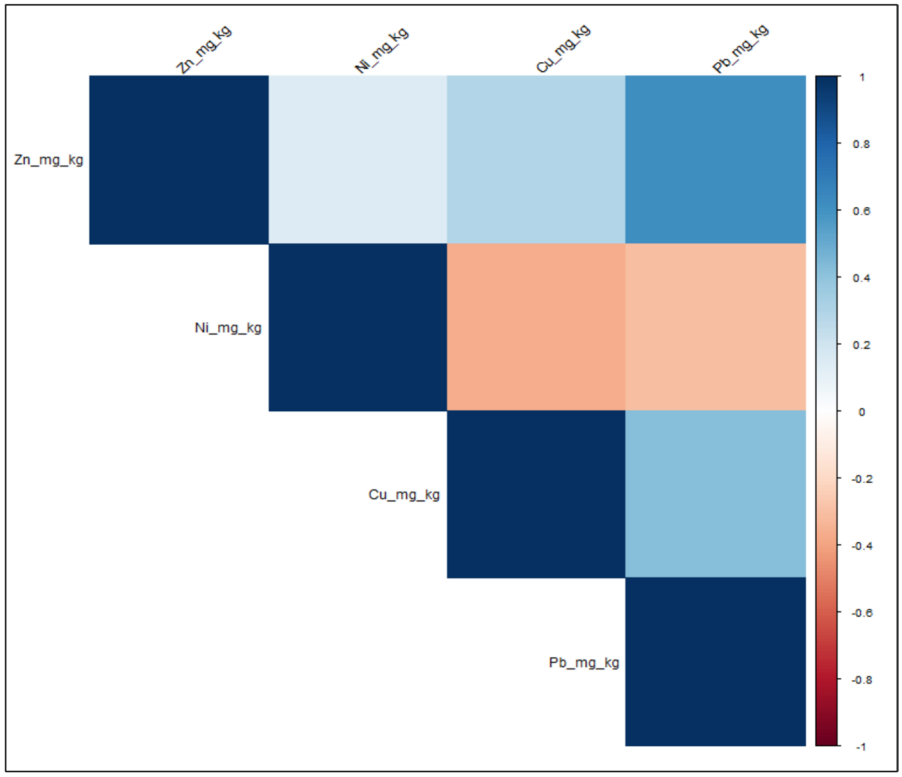

Fig. 8 Pearson correlation heatmap between heavy metals in agricultural soil samples

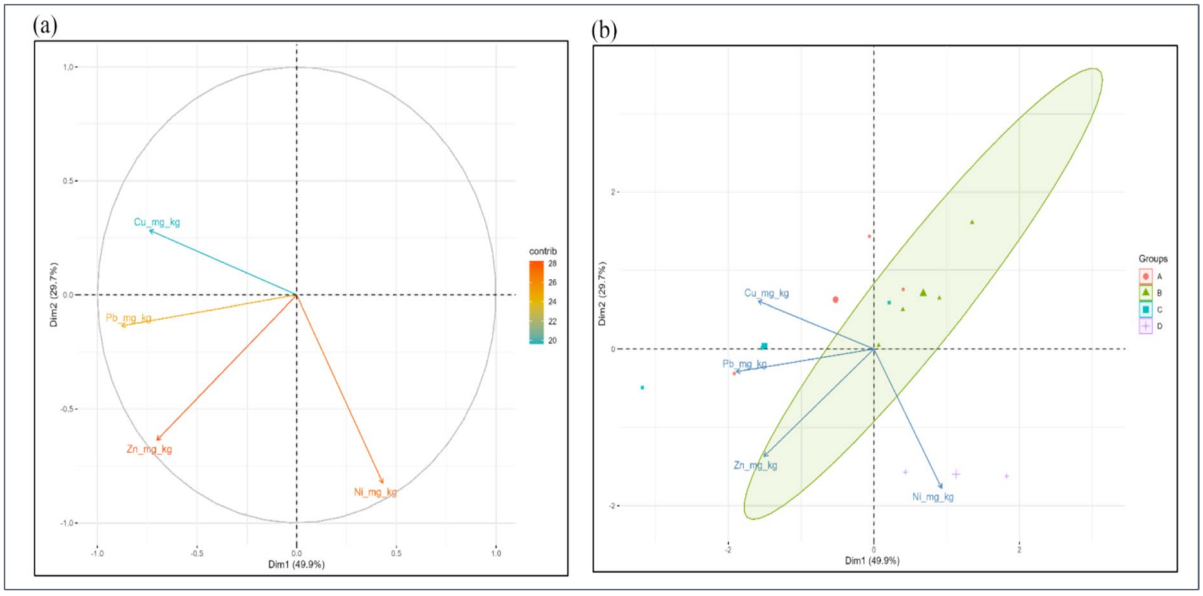

Fig. 9 PCA of the agricultural soil metal concentrations (a) Correlation circle showing the contributions of Cu, Pb, Zn, and Ni (mg/kg) to Dim1 (49.9%) and Dim2 (29.7%). (b) PCA score plot showing sample groupings (A–D) and metal loadings, with the ellipse indicating the dispersion of Group B samples

Table 5 Heavy metal concentrations (mg/kg dry weight) as the means ± SDs, HQ, and estimated CR values for selected leafy vegetables

Vegetable	Zn	Cd	Ni	Cu	Pb	HI
Okra leaves	42.77 ± 10.11	BDL	35.60 ± 1.87	3.70 ± 0.96	13.13 ± 7.44	19.38
Cowpea leaves	45.02 ± 19.12	BDL	71.33 ± 12.73	5.68 ± 2.78	12.58 ± 9.57	24.20
Pumpkin leaves	15.80 ± 8.80	BDL	16.50 ± 6.90	1.47 ± 0.45	3.30 ± 3.3	8.20
Napa Cabbage	85.00 ± 7.00	BDL	55.80 ± 4.20	9.30 ± 0.50	8.90 ± 0.30	20.64
Guideline limit	99.4[b]	0.2 –0.3[b]	67[a]	40[b]	0.1- 0.3[b]	
HQ						
Okra leaves	0.408	2.900	5.095	0.265	10.714	
Cowpea leaves	0.429	2.900	10.206	0.405	10.257	
Pumpkin leaves	0.151	2.900	2.361	0.102	2.686	
Napa Cabbage	1.810	2.900	7.975	0.665	7.286	
CR						Total CR
Okra leaves	ETE*	11×10^{-4}	0.1732	ETE*	3.2×10^{-4}	0.1732
Cowpea leaves	ETE*	11×10^{-4}	0.3469	ETE*	3.1×10^{-4}	0.3469
Pumpkin leaves	ETE*	11×10^{-4}	0.0802	ETE*	0.8×10^{-4}	0.0802
Napa Cabbage	ETE*	11×10^{-4}	0.2711	ETE*	2.2×10^{-4}	0.2711

[a](EFSA Panel on Contaminants in the Food Chain [CONTAM] et al., 2020); [b](Codex Alimentarius Commission, 2016); *ETEs are essential trace elements excluded from carcinogenic risk assessments

except for Pb (Table 5). Napa cabbage from Site D presented the highest Zn (85.0 ± 7.0 mg/kg) and Cu (9.30 ± 0.50 mg/kg) levels, whereas cowpea leaves from Site B presented peak Ni (71.3 ± 12.7 mg/kg) and Pb (12.6 ± 9.57 mg/kg) concentrations. These values are consistent with agro-mining zone reports, including Ghanaian cowpea (Pb: 14.2 mg/kg; Ni: 62.3 mg/kg; Alegbe et al., 2025) and Nigerian amaranth (Pb: 18.5 mg/kg; Ni: 70.1 mg/kg; Edogbo et al., 2020).

Statistical results are summarized in Table 5. The ANOVA results confirmed significant location-based differences for Zn ($F = 14.13$, $p < 0.001$), Ni ($F = 27.80$, $p < 0.001$), and Cu ($F = 11.53$, $p = 0.002$). Post hoc Tukey tests revealed that Site D differed significantly from all other locations for Zn and Cu, whereas the Ni concentrations were highest at Site B. Kruskal–Wallis tests supported species-level variation for Zn ($\chi^2 = 9.36$, $p = 0.025$), Ni ($\chi^2 = 10.85$, $p = 0.013$), and Cu ($\chi^2 = 10.04$, $p = 0.018$). The Cd values remained uniform across all the samples (< 0.01 mg/kg), precluding statistical testing.

The Zn levels in Napa cabbage approached the Codex Alimentarius threshold (99.4 mg/kg), which is comparable to the Zn-enriched cabbage reported by Kusznierewicz et al. (2012). The Pb concentrations in okra (13.13 mg/kg) and cowpea (12.58 mg/kg) exceeded Codex limits (0.3 mg/kg) by 43.8 times and 41.9 times, respectively, which is consistent with findings from Morogoro (Telekia, 2024) and Zanzibar (Mohammed & Khamis, 2012). Ni in cowpea surpassed the EFSA tolerable upper intake (67 mg/kg), indicating potential dietary risk. The Cd concentration remained below the detection limits, which is consistent with the findings of Nyanda and Nkuba (2017) in central Tanzania.

Correlation analysis revealed strong coaccumulation among Zn, Cu, and Ni (Fig. 10). Significant associations were observed for Zn–Cu ($r = 0.777$, $p = 0.002$), Zn–Ni ($r = 0.568$, $p = 0.043$), and Ni–Cu ($r = 0.583$, $p = 0.037$), suggesting shared uptake mechanisms or common contamination sources. The correlations between Pb and the other metals were weak ($r < 0.4$) and not statistically significant, indicating distinct accumulation behavior. Principal component analysis explained 86.7% of the total variance (Fig. 11). Dim1 (59.6%) captured enrichment patterns dominated by Zn (0.586), Cu (0.543), and Ni (0.543). Dim2 (27.1%) was defined by strong negative loading for Pb (–0.861), separating Pb-rich samples from the Zn–Cu–Ni cluster. This structure supports the correlation findings and highlights divergent contamination pathways.

The vegetable metal concentrations reflected efficient soil-to-plant transfer, particularly at Site D, where elevated soil Ni (107.20 mg/kg) corresponded with high plant uptake.

The BAF exceeded 0.1 for Zn and Pb in cowpea and Napa cabbage (Fig. 12a), suggesting species-specific accumulation behavior in polluted soils,

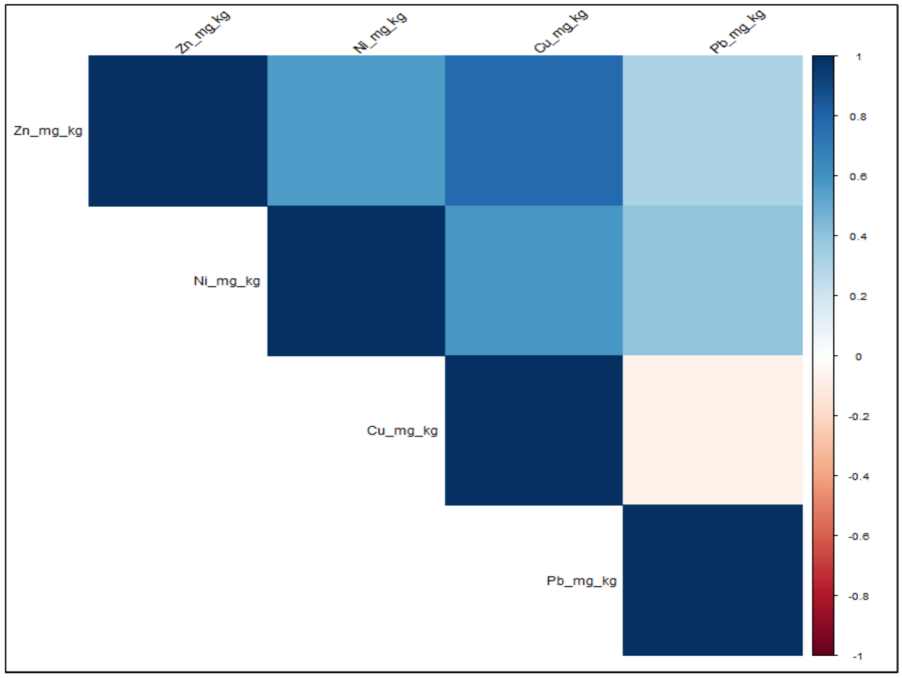

Fig. 10 Pearson correlation heatmap of heavy metal concentrations in leafy vegetables

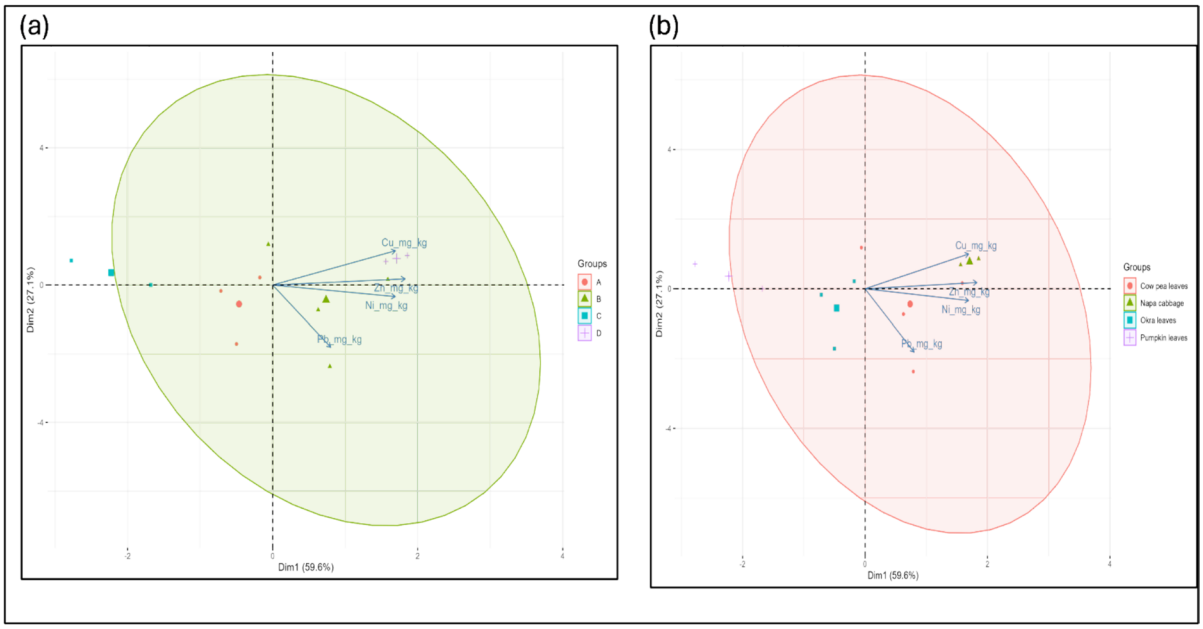

Fig. 11 PCA biplots showing (a) compositional differentiation of vegetable samples with loading vectors and confidence ellipse, and (b) sample clustering based on Cu, Zn, Ni, and Pb concentrations with loading vectors

consistent with the results of West African agro-mining studies (Alegbe et al., 2025). These patterns align with the transfer mechanisms documented near Tanzania's Mkuju uranium site (Banzi et al., 2017). These findings are consistent with direct soil-to-plant contamination, with Site D's elevated soil nickel (CF = 1.577) likely contributing to plant uptake. While root uptake from contaminated soil

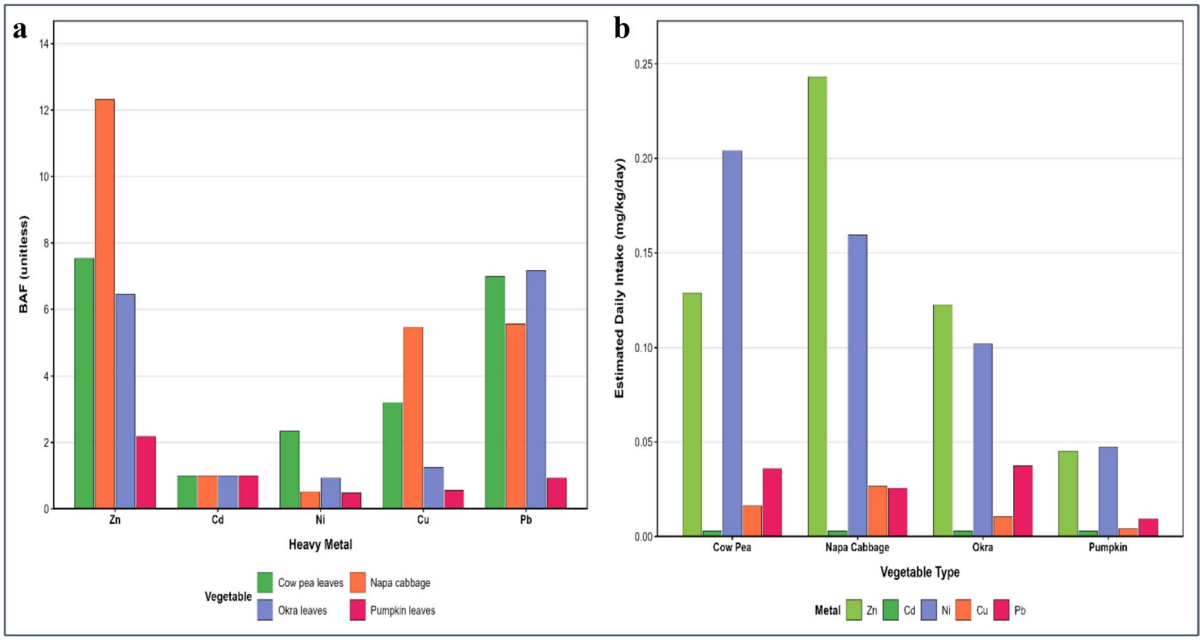

Fig. 12 Species-specific metal uptake and dietary exposure in leafy vegetables. (a) BAFs for Cd, Cu, Ni, Pb, and Zn across vegetable species (Left). (b) EDI values (mg/kg/day) for the same metals (right), highlighting dietary exposure risks

is the most probable pathway, potential contributions from foliar deposition of dust particles and irrigation water cannot be excluded without controlled uptake experiments. EDI values (Fig. 12b) highlight dietary exposure risks. Napa cabbage has elevated Zn and Cu intake, and cow pea has notable Ni intake, whereas pumpkin consistently presented the lowest EDI across all the metals.

Health risk calculations revealed significant exposure concerns (Table 5, Fig. 13). The HQ values exceeded the safety threshold (HQ > 1) for Ni and Pb in most vegetables. Cowpea presented HQs of Ni = 10.21 and Pb = 10.26, whereas Napa cabbage presented HQs of Ni = 7.98 and Pb = 7.29. The total hazard index values were highest in cowpea (24.2), followed by Napa cabbage (20.64) and okra (19.38), indicating substantial noncarcinogenic risks. Carcinogenic risks from Ni exposure in cowpea (CR = 0.347) and Napa cabbage (CR = 0.271) exceeded acceptable thresholds (1×10^{-4}), though these estimates are subject to uncertainties in consumption patterns and metal bioavailability. These findings are consistent with those reported by Rahim et al. (2024) and Kashyap and Jain (2024), who documented elevated HQ and CR values for Ni and Pb in leafy vegetables grown in river-fed agricultural areas influenced by industrial runoff.

Localized soil contamination increases dietary Ni and Pb exposure, with cowpea and napa cabbage posing the highest risks due to efficient uptake, while pumpkin leaves show lower accumulation. These findings support strategic crop selection in contaminated areas and highlight the need for comprehensive soil–plant-health evaluations. Violations of safety thresholds require interventions such as crop restrictions, soil remediation, or land-use adjustments. Diversifying crops with low-accumulating varieties may reduce exposure while preserving food security.

Conclusion

This multimedia assessment substantially achieved its objectives by quantifying heavy metal concentrations across environmental matrices during the rainy season and identifying potential pollution sources through spatial and statistical analysis in the Likuyu River catchment. While definitive source attribution would require isotopic fingerprinting or receptor modeling approaches not employed in this study,

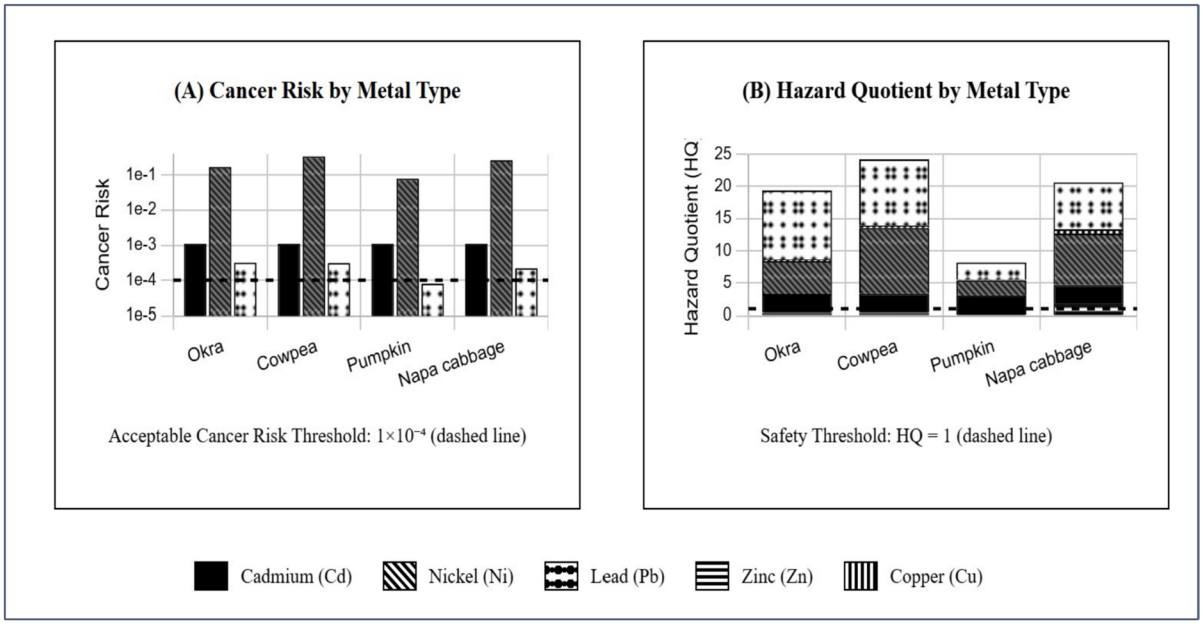

Fig. 13 Carcinogenic (CR) and noncarcinogenic (HQ) risks from metal intake in vegetables. (**A**) CR values for Cd, Ni, Pb, Zn, and Cu, with the dashed line indicating the acceptable threshold (1×10^{-4}). (**B**) HQ values for the same metals, with the dashed line representing the safety threshold (HQ = 1)

the spatial patterns and correlation analyses provide reasonable evidence for inferring dominant source contributions.

Ni and Pb were identified as the primary contaminants of concern, with elevated concentrations in specific sites and crops. Modeled health risk indices indicate possible noncarcinogenic and carcinogenic risks associated with vegetable consumption, particularly cowpea and Napa cabbage. However, these outcomes should be interpreted cautiously, given the single-season sampling design, limited spatial coverage, and reliance on estimated ingestion parameters. Future studies should include multi-seasonal sampling and expanded dietary exposure assessments to improve reliability. Despite these limitations, the study provides essential baseline data to guide environmental monitoring and agricultural management in agro-mining zones.

This study has several limitations that should be considered when interpreting the findings. Sampling was conducted only during the rainy season (April 2025), which captures peak metal mobilization but does not capture seasonal variability in concentrations, bioavailability, or exposure pathways. Dry-season conditions may show different patterns due to reduced dilution and altered sediment dynamics; hence, future investigations should include multi-seasonal sampling to assess temporal variations.

Spatial coverage was limited to five sites along a 22.7 km stretch of the river, which may not encompass all potential pollution hotspots or fully represent the catchment. The focus on surface water and topsoil (0–20 cm) excluded deeper soil and groundwater, which could serve as additional reservoirs for metals or exposure routes. Furthermore, only four commonly cultivated vegetables were analyzed, restricting the generalization of bioaccumulation and health-risk findings to other crops.

Health-risk estimates were based on standardized exposure parameters that may not accurately reflect local dietary patterns, and carcinogenic risk models did not account for variations in metal speciation or combined effects among metal mixtures. The relatively higher analytical variability in plant samples (7.6–11.8%) also reflects natural heterogeneity and may slightly affect the precision of vegetable concentration estimates.

Despite these limitations, the analytical procedures, quality controls, and complementary indices applied provide reliable evidence for identifying priority contaminants and affected sites. Immediate recommendations

include implementing targeted monitoring at identified hotspots, restricting consumption of vegetables from contaminated areas, and promoting soil remediation strategies focusing on nickel immobilization. Long-term management should integrate improved agricultural practices, pollution-source control, and community awareness to protect ecosystem integrity and food safety in mining-influenced landscapes.

Acknowledgements The authors gratefully acknowledge the financial support provided by Mbeya University of Science and Technology (MUST), which made this study possible. We extend our sincere appreciation to the residents of Likuyu-Seka Village for their cooperation and assistance during sample collection. Their support was instrumental to the success of this study. We also wish to thank the laboratory technologists at the NMAIST, GST, and TAEC laboratories for their technical expertise and invaluable assistance in the preparation and analysis of samples.

Author contributions Conceptualization – CDK, MJR, GRM, GNM, SFS; Methodology – CDK, MJR, GRM, GNM, SFS; Investigation– CDK, MJR, GRM, GNM, SFS; Writing, Original Draft Preparation: CDK; Review and Editing: MJR, GRM, GNM, SFS.

Funding This research was financially supported by the Office of the Vice Chancellor, Mbeya University of Science and Technology (MUST), Mbeya, Tanzania.

Data availability The authors confirm that all the data gathered or analyzed during this study are included in this published article.

Declarations

Ethical approval All authors have read, understood, and complied as applicable with the statement on "Ethical responsibilities of Authors" as found in the Instructions for Authors.

Consent to participate/publish All the authors gave their consent to participate in this study and gave their consent to publish this manuscript.

Competing interests The authors declare no competing interests.

Clinical trial number Not applicable.

References

Alegbe, P. J., Appiah-Brempong, M., & Awuah, E. (2025). Heavy metal contamination in vegetables and associated health risks. *Scientific African, 27*, Article e02603. https://doi.org/10.1016/j.sciaf.2025.e02603

American Public Health Association. (2022). *Standard methods for the examination of water and wastewater,* (24th ed.). American Public Health Association, American Water Works Association, Water Environment Federation.

Ashraf, I., Ahmad, F., Sharif, A., Altaf, A. R., & Teng, H. (2021). Heavy metals assessment in water, soil, vegetables and their associated health risks via consumption of vegetables, District Kasur, Pakistan. *SN Applied Sciences, 3*(5), Article 552. https://doi.org/10.1007/s42452-021-04547-y

Awuah, G. K., Mensah, J. A., & Fobil, J. N. (2020). Concentration of heavy metal in sediment, water, and fish from Ankobra and Tano River Estuaries, Ghana. *Indo Pacific Journal of Ocean Life*, *4*(2). https://doi.org/10.13057/oceanlife/o040205

Banzi, F. P. (2016). Natural radioactivity in water and its potential human health risk in the vicinity of Mkuju River Uranium Project in Tanzania. *International Journal of Environmental Protection and Policy, 4*(5), Article 111. https://doi.org/10.11648/j.ijepp.20160405.11

Banzi, F. P., Msaki, P. K., & Mohammed, N. K. (2015). Distribution of heavy metals in soils in the vicinity of the proposed Mkuju Uranium Mine in Tanzania. *Environment and Pollution, 4*(3), Article 42. https://doi.org/10.5539/ep.v4n3p42

Banzi, F. P., Msaki, P. K., & Mohammed, N. K. (2017). Assessment of radioactivity of ^{226}Ra, ^{232}Th and ^{40}K in soil and plants for estimation of transfer factors and effective dose around Mkuju River project, Tanzania. *Mining of Mineral Deposits, 11*(3), 93–100. https://doi.org/10.15407/mining11.03.093

Codex Alimentarius Commission. (2016). Report of the thirty-ninth session of the Codex Alimentarius Commission, Rome, Italy, 27 June–1 July 2016. Food and Agriculture Organization of the United Nations (FAO) and World Health Organization (WHO). IOS, 1995: update to ISO

Demsie, F., Tilahun, Y. G., & Sorsa, S. S. (2025). Assessment of potential human health risk Associated With Heavy Metals in Soil – Vegetables System Irrigated by Rift Valley Lake Ziway. Ethiopia. *Analytical Letters, 58*(4), 582–607. https://doi.org/10.1080/00032719.2024.2330487

Diarra, I. (2022). *Risk assessment of heavy metal contamination in agricultural sites and river sediments within the vicinity of an operational Gold Mine in Vatukoula, Fiji*. In Review. https://doi.org/10.21203/rs.3.rs-1512716/v1

Dinis, M. D. L., & Fiúza, A. (2021). Mitigation of uranium mining impacts—A review on groundwater remediation technologies. *Geosciences, 11*(6), Article 250. https://doi.org/10.3390/geosciences11060250

Duhan, S. S., Khyalia, P., Solanki, P., & Laura, J. S. (2023). Uranium sources, uptake, translocation in the soil-plant system and its toxicity in plants and humans: A critical review. *Oriental Journal of Chemistry, 39*(2), 303–319. https://doi.org/10.13005/ojc/390210

Edogbo, B., Okolocha, E., Maikai, B., Aluwong, T., & Uchendu, C. (2020). Risk analysis of heavy metal

contamination in soil, vegetables and fish around Challawa area in Kano State, Nigeria. *Scientific African, 7*, Article e00281. https://doi.org/10.1016/j.sciaf.2020.e00281

El Mrissani, S., Haida, S., Probst, J.-L., & Probst, A. (2021). Multi-indices assessment of origin and controlling factors of trace metals in river sediments from a semi-arid carbonated basin (the Sebou Basin, Morocco). *Water, 13*(22), 3203. https://doi.org/10.3390/w13223203

FAO/WHO. (2023). *Joint FAO/WHO Food Standards Programme Codex Committee on Contaminants in Foods* (28th, Revised eds.). FAO and WHO. https://openknowledge.fao.org/bitstreams/cdb4b110-b8bf-45dc-9c53-4ea9fcda1fc8/download. Accessed 22 Aug 2025.

Farjoudi, S. Z., & Alizadeh, Z. (2021). A comparative study of total dissolved solids in water estimation models using Gaussian process regression with different kernel functions. *Environmental Earth Sciences, 80*(17), Article 557. https://doi.org/10.1007/s12665-021-09798-x

Food and Agriculture Organization of the United Nations. (2006). *Guidelines for Soil Description* (4th ed). FAO.

Galarza, E., Moulatlet, G. M., Rico, A., Cabrera, M., Pinos-Velez, V., Pérez-González, A., & Capparelli, M. V. (2023). Human health risk assessment of metals and metalloids in mining areas of the Northeast Andean foothills of the Ecuadorian Amazon. *Integrated Environmental Assessment and Management, 19*(3), 706–716. https://doi.org/10.1002/ieam.4698

Gebreyohannes, N. M., Rwiza, M. J., Mahene, W. L., & Machunda, R. L. (2022). Assessment of contamination level of a Tanzanian river system with respect to trace metallic elements and their fate in the environment. *Water Supply, 22*(4), 3588–3602. https://doi.org/10.2166/ws.2022.002

Hakanson, L. (1980). An ecological risk index for aquatic pollution control. A sedimentological approach. *Water Research, 14*(8), 975–1001.

Hosen, A., Jahan, R. A., Simol, H. A., & Huda, M. N. (2024). Assessing heavy metal contamination in leafy vegetables and associated health risks in Dhaka, Bangladesh. *CABI Agriculture and Bioscience*, 116. https://doi.org/10.1186/s43170-024-00317-z

Hou, D., Jia, X., Wang, L., McGrath, S. P., Zhu, Y.-G., Hu, Q., Zhao, F.-J., Bank, M. S., O'Connor, D., & Nriagu, J. (2025). Global soil pollution by toxic metals threatens agriculture and human health. *Science, 388*(6744), 316–321. https://doi.org/10.1126/science.adr5214

International Organization for Standardization. (1995). ISO 5667-3: Water quality—Sampling—Part 3: Guidance on the preservation and handling of water samples. International Organization for Standardization.

Isah, M., Ameh, S., Banyigyi, H., & Tanko, D. (2024). Assessment of heavy metals in agricultural soils irrigated with water from River Kaduna, Kaduna State, Nigeria. *Confluence University Journal of Science and Technology, 1*(2), 70. https://doi.org/10.5455/CUJOSTECH.241007

Kashyap, P., & Jain, M. (2024). Concentration and non-carcinogenic risk assessment of heavy metals in leafy vegetables among different farming practices. *International Journal of Environmental Analytical Chemistry*(18). https://doi.org/10.1080/03067319.2024.2420828

Kazemi, V., Latifi, P., Darrudi, R., Ghaleh Askari, S., Mohammadi, A. A., Marufi, N., & Javan, S. (2022). Heavy metal contaminated soil, water, and vegetables in northeastern Iran: Potential health risk factors. *Journal of Environmental Health Science and Engineering, 20*(1), 65–77. https://doi.org/10.1007/s40201-021-00756-0

Kimario, I. C., Mkonda, M. Y., & Materu, S. F. (2025). Vanishing waters and growing settlements: Tracking the impact of land use land cover changes on the Lower Mara River Basin. *Wetlands Ecology and Management, 33*(5), 62. https://doi.org/10.1007/s11273-025-10080-1

Kubier, A., Wilkin, R. T., & Pichler, T. (2019). Cadmium in soils and groundwater: A review. *Applied Geochemistry, 108*, Article 104388. https://doi.org/10.1016/j.apgeochem.2019.104388

Kumar, D., & Khan, E. A. (2021). Remediation and detection techniques for heavy metals in the environment. *Heavy Metals in the Environment* (pp. 205–222). Elsevier. https://doi.org/10.1016/B978-0-12-821656-9.00012-2

Kusznierewicz, B., Bączek-Kwinta, R., Bartoszek, A., Piekarska, A., Huk, A., Manikowska, A., Antonkiewicz, J., Namieśnik, J., & Konieczka, P. (2012). The dose-dependent influence of zinc and cadmium contamination of soil on their uptake and glucosinolate content in white cabbage (*Brassica oleracea* var. *Capitata* f. *Alba*). *Environmental Toxicology and Chemistry, 31*(11), 2482–2489. https://doi.org/10.1002/etc.1977

Lemessa, F., Simane, B., Seyoum, A., & Gebresenbet, G. (2022). Analysis of the concentration of heavy metals in soil, vegetables and water around the Bole Lemi industry park, Ethiopia. *Heliyon, 8*(12), Article e12429. https://doi.org/10.1016/j.heliyon.2022.e12429

Li, K., Cui, S., Zhang, F., Hough, R., Fu, Q., Zhang, Z., Gao, S., & An, L. (2020). Concentrations, possible sources and health risk of heavy metals in multi-media environment of the Songhua River, China. *International Journal of Environmental Research and Public Health, 17*(5), 1766. https://doi.org/10.3390/ijerph17051766

Mabidi, D. M., Mutwejile, H. M., Ngweme, G. N. B., Nienie, A. B., Kayembe, J. M., Lusamba, S. N., Atibu, E. K., Carvalho, F. P., & Poté, J. (2024). Heavy metals content and ecotoxicity of sediments from the Congo River. *American Journal of Environmental Sciences, 20*(1), 64–77. https://doi.org/10.3844/ajessp.2024.64.77

MacDonald, D. D., Ingersoll, C. G., & Berger, T. A. (2000). Development and evaluation of consensus-based sediment quality guidelines for freshwater ecosystems. *Archives of Environmental Contamination and Toxicology, 39*(1), 20–31. https://doi.org/10.1007/s002440010075

Mataba, G. R., Verhaert, V., Blust, R., & Bervoets, L. (2016). Distribution of trace elements in the aquatic ecosystem of the Thigithe river and the fish *Labeo victorianus* in Tanzania and possible risks for human consumption. *Science of the Total Environment, 547*, 48–59. https://doi.org/10.1016/j.scitotenv.2015.12.123

Mdachi, D. D., Rugaika, A. M., & Machunda, R. L. (2024). The assessment of heavy metals and natural radioactivity in the phosphate tailings at Minjingu Mines in Tanzania.

Journal of Ecological Engineering, 25(1), 269–277. https://doi.org/10.12911/22998993/175249

Mitra, S., Chakraborty, A. J., Tareq, A. M., Emran, T. B., Nainu, F., Khusro, A., Idris, A. M., Khandaker, M. U., Osman, H., Alhumaydhi, F. A., & Simal-Gandara, J. (2022). Impact of heavy metals on the environment and human health: Novel therapeutic insights to counter the toxicity. *Journal of King Saud University - Science, 34*(3), Article 101865. https://doi.org/10.1016/j.jksus.2022.101865

Mohammed, N. K., & Khamis, F. O. (2012). Assessment of heavy metal contamination in vegetables consumed in Zanzibars. *Natural Science, 04*(08), 588–594. https://doi.org/10.4236/ns.2012.48078

Mohammed, N. K., & Mazunga, M. S. (2013). Natural radioactivity in soil and water from Likuyu Village in the neighborhood of Mkuju Uranium Deposit. *International Journal of Analytical Chemistry, 2013*, 1–4. https://doi.org/10.1155/2013/501856

Mohammed, N., & Nkuba, L. (2017). Concentration Levels and the Associated Health Risks of Elements in Food Crops Grown in the Neighbourhood of Minjingu Phosphate Mine, Tanzania. Chemical Science International Journal, 18(1), 1–9.https://doi.org/10.9734/CSJI/2017/31476

Müller, G. (1979). Schwermetalle in den Sedimenten des Rheins-Veränderungen seit 1971. *Umschau in Wissenschaft und Technik, 79*, 778–783.

Mustatea, G., Ungureanu, E. L., Iorga, S. C., Ciotea, D., & Popa, M. E. (2021). Risk assessment of lead and cadmium in some food supplements available on the Romanian market. *Foods, 10*(3), 581. https://doi.org/10.3390/foods10030581

Njoki, S., Omar Hashim, N., & Chege, M. (2024). Evaluation of Heavy Metal Concentration in Sediments of Rupingazi River, Kenya. *International Journal of Innovative Science and Research Technology (IJISRT)*, 647–653. https://doi.org/10.38124/ijisrt/IJISRT24SEP002.

Nkinda, M. S., Rwiza, M. J., Ijumba, J. N., & Njau, K. N. (2021). Heavy metals risk assessment of water and sediments collected from selected river tributaries of the Mara River in Tanzania. *Discover Water, 1*(1), 3. https://doi.org/10.1007/s43832-021-00003-5

Nur-E-Alam, M., Salam, M. A., Dewanjee, S., Hasan, M. F., Rahman, H., Rak, A. E., Islam, A. R. M. T., & Miah, M. Y. (2022). Distribution, concentration, and ecological risk assessment of trace metals in surface sediment of a tropical Bangladeshi urban river. *Sustainability, 14*(9), 5033. https://doi.org/10.3390/su14095033

Nyanda, P., & Nkuba, L. (2017). Natural radioactivity in vegetables from selected areas of Manyoni District in central Tanzania. *Physical Science International Journal, 16*(2), 1–10. https://doi.org/10.9734/PSIJ/2017/34746

Osae, R., Nukpezah, D., Darko, D. A., Koranteng, S. S., & Mensah, A. (2023). Accumulation of heavy metals and human health risk assessment of vegetable consumption from a farm within the Korle lagoon catchment. *Heliyon, 9*(5), Article e16005. https://doi.org/10.1016/j.heliyon.2023.e16005

Pal, D., & Maiti, S. K. (2018). Seasonal variation of heavy metals in water, sediment, and highly consumed cultured fish (*Labeo rohita* and *Labeo bata*) and potential health risk assessment in aquaculture pond of the coal city, Dhanbad (India). *Environmental Science and Pollution Research, 25*(13), 12464–12480. https://doi.org/10.1007/s11356-018-1424-5

Rahi, D. C., Chandak, R., & Vishwakarma, A. (2024). Assessment of seasonal fluctuation in heavy metal contamination in sediments and surface water of Narmada River, India. *Journal of Water and Climate Change, 15*(7), 3173–3189. https://doi.org/10.2166/wcc.2024.071

Rahim, N., Noor, A., Kanwal, A., Tahir, M. M., & Yaqub, A. (2024). Assessment of heavy metal contamination in leafy vegetables: Implications for public health and regulatory measures. *Environmental Monitoring and Assessment, 196*(8), 684. https://doi.org/10.1007/s10661-024-12855-0

Rajesh, M., & Rehana, S. (2022). Impact of climate change on river water temperature and dissolved oxygen: Indian riverine thermal regimes. *Scientific Reports, 12*(1), 9222. https://doi.org/10.1038/s41598-022-12996-7

Romero-Estévez, D., Yánez-Jácome, G. S., Simbaña-Farinango, K., & Navarrete, H. (2019). Distribution, contents, and health risk assessment of cadmium, lead, and nickel in Bananas Produced in Ecuador. *Foods, 8*(8), 330. https://doi.org/10.3390/foods8080330

Royal Botanic Gardens, Kew. (2025). Vigna unguiculata (L.) Walp. | Plants of the World Online | Kew Science. Plants of the World Online. https://powo.science.kew.org/taxon/urn:lsid:ipni.org:names:1127257-2

Sawe, S. F., Shilla, D. A., & Machiwa, J. F. (2021). Lead (Pb) contamination trends in Msimbazi estuary reconstructed from 210Pbdated sediment cores (Msimbazi River, Tanzania). Environmental Forensics, 22(1–2), 99–107. https://doi.org/10.1080/15275922.2020.1805823

Sabijon, J., Ultra, V., Openiano, M., Bollido, M., Poliquit, D., Aquino, R., Espejon Jr., E., Tan, Z. N., & Bejar, F. (2024). Nutrients and heavy metal contents on surface of agricultural soils in the flood-plains of Taft River Basin impacted by Bagacay Mines, Philippines. *Philippine Journal of Science*, *153*(1). https://doi.org/10.56899/153.01.32

Said, S., Benazzouz, B., Bounouira, H., Amsil, H., & Moussaif, A. (2025). Comprehensive analysis of heavy metals content in organic and conventional vegetables and their health risk assessment. *International Journal of Environmental Analytical Chemistry*, 1–17. https://doi.org/10.1080/03067319.2025.2463998

Saleem, M., Pierce, D., Wang, Y., Sens, D. A., Somji, S., & Garrett, S. H. (2024). Heavy metal(oid)s contamination and potential ecological risk assessment in agricultural soils. *Journal of Xenobiotics, 14*(2), 634–650. https://doi.org/10.3390/jox14020037

Sanga, V., & Pius, F. (2024). Heavy metal contamination in soil and food crops and associated human health risks in the vicinity of Iringa Municipal dumpsite, Tanzania. *Discover Environment, 2*(1), Article 104. https://doi.org/10.1007/s44274-024-00137-y

EFSA Panel on Contaminants in the Food Chain (CONTAM), Schrenk, D., Bignami, M., Bodin, L., Chipman, J. K., del Mazo, J., Grasl-Kraupp, B., Hogstrand, C., Hoogenboom,

L. (Ron), Leblanc, J., Nebbia, C. S., Ntzani, E., Petersen, A., Sand, S., Schwerdtle, T., Vleminckx, C., Wallace, H., Guérin, T., Massanyi, P., … Nielsen, E. (2020). Update of the risk assessment of nickel in food and drinking water. *EFSA Journal, 18*(11). https://doi.org/10.2903/j.efsa.2020.6268

Silas, E. N., Ombaka, O., Chomba, E., & Muraya, M. (2024). Assessment of heavy metal pollution in water and sediment of River Thiba, Kirinyaga County, Kenya. *International Journal of Advances in Scientific Research and Engineering, 10*(08), 74–84. https://doi.org/10.31695/IJASRE.2024.8.9

Srivastava, R. R., Pathak, P., & Perween, M. (2020). Environmental and Health Impact Due to Uranium Mining. In D. K. Gupta & C. Walther (Eds.),

Tanzania Bureau of Standards. (2007). Environmental Management (Soil Quality Standards) Regulations, 2007. Government of Tanzania.

Telekia, F. A. (2024). Assessment of concentration levels and associated health risks of arsenic, c, lead, and mercury in selected green leafy vegetables irrigated by Morogoro River using atomic absorption spectroscopy. *East African Journal of Environment and Natural Resources, 7*(2), 35–47. https://doi.org/10.37284/eajenr.7.2.2292

Turekian, K. K., & Wedepohl, K. H. (1961). Distribution of the elements in some major units of the earth's crust. *Geological Society of America Bulletin, 72*(2), 175–192.

United States Environmental Protection Agency. (2011). Exposure factors handbook: 2011 edition (EPA/600/R-09/052F). National Center for Environmental Assessment, Office of Research and Development, U.S. Environmental Protection Agency.

United States Environmental Protection Agency. (1996). Method 3050B: Acid digestion of sediments, sludges, and soils (Revision 2). U.S. Environmental Protection Agency.

Wang, Y., Li, B., Zhu, J., Feng, Q., Liu, W., He, Y., & Wang, X. (2022). Assessment of heavy metals in surface water, sediment and macrozoobenthos in inland rivers: A case study of the Heihe River, Northwest China. *Environmental Science and Pollution Research, 29*(23), 35253–35268. https://doi.org/10.1007/s11356-022-18663-8

Wedepohl, K. H. (1995). The composition of the continental crust. *Geochimica et Cosmochimica Acta, 59*(7), 1217–1232. https://doi.org/10.1016/0016-7037(95)00038-2

WHO. (2022). *Guidelines for drinking-water quality (Fourth edition incorporating the first and second addenda)*. World Health Organization.

Zhang, X., Liu, X., & Zhan, C. (2024). Emerging contaminants in aquatic ecosystems: Sources, effects, and mitigation approaches. *International Journal of Aquaculture*. https://doi.org/10.5376/ija.2024.14.0023